Molecular Biology of the Cell
Vol. 3, 633–654, June 1992

The Yeast Ca^{2+}-ATPase Homologue, PMR1, is Required for Normal Golgi Function and Localizes in a Novel Golgi-like Distribution

Adam Antebi and Gerald R. Fink

Whitehead Institute of Biomedical Research and Department of Biology, Massachusetts Institute of Technology, Cambridge, Massachusetts 02142

Submitted February 7, 1992; Accepted April 22, 1992

PMR1, a Ca^{2+}-adenosine triphosphatase (ATPase) homologue in the yeast *Saccharomyces cerevisiae* localizes to a novel Golgi-like organelle. Consistent with a Golgi localization, the bulk of PMR1 comigrates with Golgi markers in subcellular fractionation experiments, and staining of PMR1 by indirect immunofluorescence reveals a punctate pattern resembling Golgi staining in yeast. However, PMR1 shows only partial colocalization with known Golgi markers, KEX2 and SEC7, in double-label immunofluorescence experiments. The effect of PMR1 on Golgi function is indicated by pleiotropic defects in various Golgi processes in *pmr1* mutants, including impaired proteolytic processing of pro-α factor and incomplete outer chain glycosylation of invertase. Consistent with the proposed role of PMR1 as a Ca^{2+} pump, these defects are reversed by the addition of millimolar levels of extracellular Ca^{2+}, suggesting that Ca^{2+} disposition is essential to normal Golgi function. Absence of PMR1 function partially suppresses the temperature-sensitive growth defects of several *sec* mutants, and overexpression of PMR1 restricts the growth of others. Some of these interactions are modulated by changes in external Ca^{2+} concentrations. These results imply a global role for Ca^{2+} in the proper function of components governing transit and processing through the secretory pathway.

INTRODUCTION

The organelles of the secretory pathway play a critical role in the control of cellular Ca^{2+}. In addition to their function in sorting, post-translational modification, and transit of secreted, vacuolar, and lysosomal proteins, many of these membrane-bound compartments also serve as intracellular Ca^{2+} reservoirs. The endoplasmic reticulum (ER)[1] contains high levels of Ca^{2+} (Somlyo *et al.*, 1985) that are released during inositol-1,4,5-trisphosphate (IP_3)-mediated signal transduction (Streb *et al.*, 1984). The Ca^{2+} content of the Golgi and downstream secretory vesicles in some cell types is substantial (Roos, 1988). Whether organelles of the secretory pathway utilize Ca^{2+} gradients for aspects of secretion or whether these compartments act simply as storehouses for Ca^{2+} is not clear.

Ca^{2+} is known to affect diverse functions within the secretory pathway. Ca^{2+} influx across the plasma membrane or release from intracellular stores triggers the exocytosis of secretory granules in many cell types (Burgoyne, 1987), a late step in regulated secretion. A critical Ca^{2+} concentration is required for ER to Golgi (Beckers and Balch, 1989; Baker *et al.*, 1990), inter-Golgi (Schwaninger *et al.*, 1991), and post-Golgi in vitro transport reactions in some cell types (deCurtis and Simons, 1988). Perturbation of lumenal Ca^{2+} concentrations in the ER have been suggested to influence the retention of resident lumenal proteins (Booth and Koch, 1989), affect protein folding (Lodish and Kong, 1990), promote protein degradation (Wileman *et al.*, 1991), and regulate the association of immunoglobulin heavy chain binding protein (BiP) with misfolded proteins (Suzuki *et al.*, 1991). Within trans-Golgi compartments and secretory granules, Ca^{2+} is thought to participate in concentration and packaging of components by catalyzing the aggregation of secretogranins (for review, see Huttner *et al.*, 1991).

Events governed by Ca^{2+} universally depend on a steep Ca^{2+} gradient established across membranes, with cytosolic Ca^{2+} lowered to submicromolar concentrations

[1] Abbreviations used: CPY, carboxypeptidase Y; ER, endoplasmic reticulum; GDPase, guanosinediphosphatase; PM, plasma membrane; SR, sarcoplasmic reticulum.

and the lumenal Ca^{2+} content of compartments elevated to millimolar levels (Carafoli, 1987). This asymmetric distribution is achieved in part by P-type Ca^{2+}-pumping adenosine triphosphatases (ATPases), which couple ATP hydrolysis to the unidirectional removal of Ca^{2+} from the cytosol (Carafoli, 1987). In mammalian cells, three related classes of Ca^{2+}-ATPases have been defined, which differ slightly in their structural and biochemical parameters: 1) plasma membrane Ca^{2+} pumps, which are responsive to calmodulin and extrude Ca^{2+} out of the cell (for review, see Carafoli 1991); 2) sarco/endoplasmic reticulum Ca^{2+}-ATPases, which sequester Ca^{2+} within intracellular compartments (MacLennan *et al.*, 1985; Gunteski-Hamblin *et al.*, 1988; Burk *et al.*, 1989); and 3) a relatively uncharacterized third class of presumed Ca^{2+}-ATPase that displays features distinct from plasma membrane and sarco/endoplasmic pumps, expressed in many cell types (Gary Shull, unpublished observations). We have previously identified a Ca^{2+}-ATPase homologue in the yeast *Saccharomyces cerevisiae* called *PMR1* (Rudolph *et al.*, 1989), which belongs to this third class of Ca^{2+}-ATPases because its deduced amino acid sequence demonstrates 50% identity with the human gene (Gary Shull, unpublished observations). In addition to the well-characterized Ca^{2+} pumps resident in the membranes of the sarco/endoplasmic reticulum and the plasmalemma, Ca^{2+}-uptake activity or proteins antigenically related to Ca^{2+} pumps have been localized to the Golgi apparatus (Virk *et al.*, 1985), lysosomes (Klemper, 1985), secretory granules (King *et al.*, 1988), endocytic compartments (Milne and Coukell, 1989) and calciosomes (Volpe *et al.*, 1988). The genes encoding these pumps have not been assigned nor are the physiological functions of pumps within these diverse compartments known.

A genetic approach toward understanding the cellular role of Ca^{2+}-pumping ATPases enables direct observation of the in vivo consequences of perturbing Ca^{2+} sequestration in particular Ca^{2+} pools. The phenotypes of *pmr1* mutant strains implicate a functional role for this class of Ca^{2+}-ATPase in secretory protein transport and processing (Rudolph *et al.*, 1989): strains carrying a *pmr1* deletion secrete heterologous yeast/mammalian secretory proteins normally retained internally in wild-type strains, manifest a glycosylation defect, and suppress a cold-sensitive lesion in YPT1, a Golgi-associated GTP binding protein involved in ER/Golgi transit (Segev *et al.*, 1988; Bacon *et al.*, 1989; Baker *et al.*, 1990).

Given the diversity of Ca^{2+}-ATPases, the localization of a particular pump could give important clues to its cellular function. To determine the organelle that is altered in *pmr1* strains and to clarify the physiology of mutant phenotypes, we have localized the *PMR1* gene product. In this work, we show that the PMR1 protein localizes in a Golgi-like distribution, and we pinpoint *pmr1*-induced secretory dysfunction to the Golgi apparatus.

MATERIALS AND METHODS

Media and Strain Construction

Yeast growth in standard media (Difco, Detroit, MI), sporulation, tetrad dissection, and strain maintenance were carried out as described in Sherman *et al.*, (1986). Synthetic low Ca^{2+} media were prepared as described previously (Rudolph *et al.*, 1989). The Ca^{2+} concentration of YPD is estimated to be relatively low (~180 μM, Ohya *et al.*, 1984) and was supplemented with $CaCl_2$ where indicated. Strains were transformed by the lithium acetate method (Ito *et al.*, 1983). Most AA series strains are derived from AA255, a strain equivalent to N170 (R. Young, M.I.T.). This strain arose as an ascospore from a cross between DBY1826 (D. Botstein, Stanford U.) and JY380 (G. Fink). ER/Golgi *sec* mutants (strains AA460, 465, 466, 468, 471, 473, 474, 476, 479, and 480) came from crosses between AA255 and RSY265-282 series (Kaiser and Schekman, 1990). AA577, the strain harboring an integrated *PMR1::HA* fusion allele, was constructed by transforming AA274 with the 8.1 kb *Aat* II fragment from pL149/N13 in a one-step gene replacement experiment (Rothstein, 1983); transformants were selected for growth on low Ca^{2+} media. Leu− strains were those in which *pmr1-1::LEU2* had been replaced by *PMR1::HA* as confirmed by Southern blot analysis. AA577 was put through a cross to yield isogenic sister spores carrying *PMR1::HA*, which were subsequently mated to give the diploid AA662. AA662 was converted to isogenic a/a and α/α diploids utilizing the galactose-inducible HO plasmid, and the resultant strains were mated to form the tetraploid AA654, harboring four copies of *PMR1::HA*. Table 1 contains a list of the strains used in this work.

DNA Manipulations and Plasmids

Most DNA manipulations were carried out as outlined in Maniatas *et al.* (1982). Preparation of single-stranded DNA from phagemids was performed according to Vieira and Messing (1987). Bacterial transformation was carried out with the Hanahan procedure (1985). The following is a description of plasmids used in this work.

1) pL129 is a multiple copy 2μ vector containing the 8.1-kb *Aat* II fragment of the complete *PMR1* gene (Rudolph *et al.*, 1989) cloned into the *Aat* II site of YEp24.

2) pL144 is a *trpE::PMR1* fusion in which *Escherichia coli trpE* is fused to the C-terminal 1.75-kb *Hin*dIII fragment of *PMR1* (nucleotides 4592–6340 from published sequence, Rudolph *et al.* (1989), in the vector *pATH11* (Koerner *et al.*, 1991).

3) pL148 was constructed from pUN80 (Elledge and Davis, 1988), by placing *Aat* II linkers via blunt-end ligation into the *Sma* I site of the pUN80 polylinker. This multipurpose shuttle plasmid served as the *URA3* marked *CEN* backbone for pL149 and pL149/N13. The M13 origin also enabled the production of ssDNA as a template for site-directed insertion mutagenesis (see below).

4) pL149 was constructed by ligating the 8.1-kb *Aat* II fragment containing *PMR1* into the *Aat* II site of pL148.

5) pL149/N13 contains the epitope-tagged derivative of *PMR1::HA* in the pL148 backbone (see *Epitope Tagging*).

6) pL161, a 2μ plasmid bearing the *PMR1::HA* fusion protein, was made by cloning the 8.1-kb *Aat* II fragment from pL149/N13 into the *Aat* II site of YEp24.

7) pYCpKX212 contains *KEX2* expressed from the *TDH3* promoter in YCp50 (Redding *et al.*, 1991).

Epitope Tagging

Epitope tagging was performed according to Kolodziej and Young (1991) using site-directed insertion mutagenesis (Kunkel *et al.*, 1987) to introduce nucleotides encoding a nine amino acid epitope from the influenza virus hemagglutinin protein, YPYDVPDYA (Wilson *et al.*, 1984) into *PMR1*. A synthetic 64-base oligo bearing 27 nucleotides encoding the flu epitope, flanked on the 5′ side by 17 bases and on the 3′ side by 20 bases of complementary *PMR1* DNA (sequence AAGATAAGATAATTATGTACCCATACGACGTTCCAGACTAC-

GCTAGCGACAATCCATTTAATGC) was used to perform insertion mutagenesis on single-stranded pL149 carrying the *PMR1* gene. Successful insertion was determined by screening plasmid DNAs for a novel *Nhe*I restriction site created at the 3' *PMR1::HA* fusion joint, and the mutagenesis was confirmed by DNA sequencing (Sanger *et al.*, 1977). The epitope was inserted directly after the amino terminal ATG codon of *PMR1* at position 2714 (numbering from Rudolph *et al.*, 1989).

Genetic Interaction of pmr1-1 and PMR1 2μ with sec Mutants

Suppression was analyzed by mating *sec leu2 ura3* strains listed in Table 1 to *pmr1-1::LEU2* and isogenic *PMR1* strains. Diploids were sporulated, and the resulting ascospores from both experimental and control crosses were dissected onto the same YPD plate at the permissive temperature, 24°C. Tetrads were replica plated to YPD, and the replicas were incubated at 24, 28, 30, 32, 34, 36, 37, and 38°C. Analysis of phenotypes in this range gave a broad window within which suppression could be observed and permitted the unambiguous assignment of *sec* mutant genotype by phenotypic testing at these various temperatures. Plates were scored at 1, 2, and 3 d. Suppression was evident in those *pmr1* × *sec* crosses, which gave 2:2, 3:1, and 4:0 ascospore viability patterns, whereas only 2:2 viability patterns were usually seen in control crosses to wild type under identical conditions. Suppression was shown to be linked to *pmr1-1::LEU2* in further outcrosses of the *pmr1 sec* double mutants to *sec* single mutants and/or wild-type strains. Isogenic *sec* and *sec pmr1* strains were constructed by transforming *pmr1 sec* double mutants (strains AA688, 691, 696, 697, 710, 716) with either *PMR1* on a single-copy plasmid (pL149) or a control plasmid (pUN80). Isogenic strains were scored for their ability to grow at the nonpermissive temperature on YPD and SC-ura plates. Suppression of *pmr1 sec6-4* and *pmr1 sec19-1* was clear on SC-ura medium. Suppression of *pmr1 sec15-1* was weak on YPD plates and was not evident on SC-ura.

For examining the effects of *PMR1* overexpression on *sec* mutants, *sec* mutant strains (Table 1) were transformed with YEp24, pL149, and pL129 plasmids. Two YEp24, two pL149, and two to four pL129 transformants were analyzed for genetic interaction. For each set of *sec* strain derivatives, equal numbers of logarithmically growing cells were serially diluted into 96-well microtiter dishes, and cultures were transferred onto SC-ura plates with a multipronged inoculator. The replicas were incubated at 22, 28, 30, 32, 34, 36, 37, and 38°C, and phenotypes were scored after 1, 2, and 3 d. For *ypt1-1* (cs) strains, the permissive temperature is 30°C. Derivative strains were transferred with a replica inoculator and incubated at 30, 28, 24, 22, 18, and 14°C.

Anti-TrpE::PMR1 Antibodies

A carboxy terminal fusion of *PMR1* to *E. coli trpE* (pL144) encoding a TrpE::PMR1 fusion protein was induced in *E. coli* with indolacrylic acid according to Koerner *et al.* (1991). Protein extracts for soluble and insoluble fractions were prepared according to Spindler *et al.* (1984). The TrpE::PMR1 fusion protein was found primarily in the insoluble fraction. Preparative amounts of the fusion protein were purified by separating extracts through sodium dodecyl sulfate-polyacrylamide gel electrophoresis (SDS-PAGE) and obtaining the fusion protein from gel slices as described by Davis and Fink (1990). Immunization and bleeding of mice were carried out according to Davis and Fink (1990).

Protein Extracts

For immunoblot analysis of PMR1, protein extracts were prepared by glass bead rupture in 10% trichloroacetic acid according to Ohashi *et al.* (1982). The pellet was resuspended in 10–20 μl 100 mM tris(hydroxymethyl)amino methane (Tris) base at 4°C and solubilized in Laemmli's sample buffer (Laemmli, 1970) at 55–60°C for 5 min before SDS-PAGE. Invertase extracts were prepared as described (Schauer *et al.*, 1985). Endoglycosidase H treatment was carried out according to Orlean *et al.* (1991).

SDS-PAGE, Western Blotting, and Quantitation of Autoradiograms

Samples were resolved by SDS-PAGE using a modified Laemmli system (Laemmli, 1970) in which SDS is omitted from the gel and lower electrode buffer. For the analysis of electrophoretically resolved ^{35}S-labeled proteins, gels were fixed, prepared for fluorography, and exposed autoradiographically as described (Rothblatt *et al.*, 1989). Western blotting was carried out essentially as outlined by Johnson *et al.* (1984) with the use of 0.05–0.2% Tween 20 for the detergent phase in all buffers. Primary antibodies were used at the following dilutions: anti-HA mouse monoclonal 12CA5, 1:50 (Field *et al.*, 1988); polyclonal mouse anti-TrpE::PMR1 antisera, 1:250; guinea pig anti-invertase antisera (the kind gift of Daphne Preuss, Stanford U.), 1:2500; anti-PMA1 mouse monoclonal F10-9 from monoclonal supernatants (kindly provided by John Teem), diluted 1:4 in phosphate-buffered saline (PBS), 0.2% Tween 20; affinity purified anti-DPM1 rabbit antisera (kindly provided by Peter Orlean, U. Illinois, Urbana), 1:100; and rabbit anti-KAR2 antisera (the gift of Mark Rose, Princeton U.), 1:5000. Washed blots carrying bound primary rabbit antibodies were incubated 1–2 h with [^{125}I]-Protein A and washed as described (Johnson *et al.*, 1984). To visualize bound mouse antibodies, washed blots with bound mouse antibodies were incubated 1–2 h with affinity-purified rabbit anti-mouse IgG diluted 1:1000 (Jackson Immunoresearch, West Grove, PA), washed, and then incubated with [^{125}I]-Protein A and washed again. Filters were placed against preflashed Kodak XAR 5 film and exposed at −70°C with an intensifying screen. Quantitation of autoradiograms was carried out with a Molecular Dynamics scanner (Molecular Dynamics, Sunnyvale, CA) furnished with Image-quant software.

Cell Growth, Radiolabeling, and Immunoprecipitation

Yeast growth in low-sulfate synthetic medium, invertase induction, and pulse labeling were carried out essentially as described by Rothblatt *et al.* (1989). $CaCl_2$ was excluded from the medium and supplemented to 1 mM $CaCl_2$ unless noted otherwise. Immunoprecipitation of carboxypeptidase (CPY) and alpha factor was carried out by the methods of Rothblatt *et al.* (1989). Immunoprecipitation of invertase was performed essentially according to Rothblatt *et al.* (1989) except that immunoprecipitation was carried out in immunoprecipitation (IP) buffer (PBS, 1% Triton X-100, 0.1% SDS). Successive washes were carried out in 1) IP buffer plus 2 M Urea, 2) IP buffer plus 300 mM NaCl, and 3) 50 mM NaCl, 10 mM Tris-HCl, pH 7.5. Mannose linkages on invertase were characterized as described by Franzusoff and Schekman (1989). For pulse-chase analysis of invertase, cultures of AA274 and AA255 were induced for invertase synthesis, pulsed-labeled for 5 min at 21°C with 60-μCi tran-^{35}S-label (ICN Radiochemicals, Irvine, CA) per optical density 600 (OD_{600}) U and chased as described (Rothblatt *et al.*, 1989). Aliquots (1 OD_{600} equivalent) were withdrawn at 0, 1, 2, 3, 4, 6, 8, 12, 20, and 40 min after the chase. Cells were separated into periplasmic and cellular fractions and solubilized as described (Schauer *et al.*, 1985). Invertase was immunoprecipitated from the samples under denaturing conditions and resolved by SDS-PAGE in 7.5% polyacrylamide gels.

Immunofluorescence

Staining of fixed yeast cells by indirect immunofluorescence was carried out essentially according to Davis and Fink (1990), with fixation typically carried out on ice for 2 h. Double-labeling experiments with PMR1::HA as one antigen and various other antigens were carried out with both primary antibodies simultaneously present in primary incubations and both secondary antibodies concommitantly present in secondary incubations. Primary antisera were diluted as follows: 12CA5 from ascites fluid, 1:250; crude anti-KAR2 antisera, 1:5000

Table 1. Strain list

Strain	Genotype	Source
AA255	*MATα ade2 his3Δ200 leu2-3,112 lys2Δ201 ura3-52*	R. Young (M.I.T.)
AA274	*MATα pmr1-1::LEU2 ade2 his3Δ200 leu2-3,112 lys2Δ201 ura3-52*	This work
AA277	*MATα ade2 leu2-3,112 lys2Δ201 ura3-52*	This work
AA280	*MATα ade2 his3Δ200 lys2Δ201 ura3-52*	This work
AA288	*MATa ade2 leu2-3,112 lys2Δ201 ura3-52*	This work
AA291	*MATa ade2 his3Δ200 lys2Δ201 ura3-52*	This work
AA298	*MATα pmr1-1::HIS3 ade2 his3Δ200 leu2-3,112 lys2Δ201 ura3-52*	This work
AA300	*MATa pmr1-1::LEU2 ade2 his3Δ200 leu2-3,112 lys2Δ201 ura3-52*	This work
AA305	(AA291/AA277) *MATa/MATα ade2/ade2 his3Δ200/+ +/leu2-3,112 lys2Δ201/lys2Δ201 ura3-52/ura3-52*	This work
AA311	*MATα ypt1-1*(cs) *leu2-3,112 lys2 ura3-52*	This work
AA401	*MATa pmr1-1::LEU2 ypt1-1 ACT1*::pRB151 *(URA3) his3Δ200 leu2-3,112 lys2 ura3-52*	This work
AA402	*MATα ypt1-1 ACT1*::pRB151 *(URA3) leu2-3,112 lys2 ura3-52*	This work
AA459	*MATa sec18-1 leu2-3,112 lys2Δ201 ura3-52*	This work
AA460	*MATα sec18-1 ade2 leu2-3,112 lys2Δ201 ura3-52*	This work
AA465	*MATa sec22-3 leu2-3,112 ura3-52*	This work
AA466	*MATa sec21-1 ade2 his3Δ200 leu2-3,112 ura3-52*	This work
AA468	*MATα sec19-1 his3Δ200 leu2-3,112 lys2Δ201 ura3-52*	This work
AA471	*MATa sec12-4 leu2-3,112 ura3-52*	This work
AA473	*MATa sec13-1 leu2-3,112 lys2Δ201 ura3-52*	This work
AA474	*MATa sec16-2 his3 leu2-3,112 lys2Δ201 ura3-52*	This work
AA476	*MATa sec17-1 his3 leu2-3,112 ura3-52*	This work
AA479	*MATa sec20-1 leu2-3,112 lys2Δ201 ura3-52*	This work
AA480	*MATa sec23-1 ade2 leu2-3,112 ura3-52*	This work
AA482	*MATa sec7 ade2 his3Δ200 leu2-32,112 lys2Δ201 ura3-52*	This work
AA522	(AA274/AA300) *MATα/MATa pmr1-1::LEU2/pmr1-1::LEU2 ade2/ade2 his3Δ200/his3Δ200 leu2-3,112/ leu2-3,112 lys2Δ201/lys2Δ201 ura3-52/ura3-52*	This work
AA530	AA522(pL161)	This work
AA577	*MATα PMR1::HA ade2 his3Δ200 leu2-3,112 lys2Δ201 ura3-52*	This work
AA654	*MATα/MATα/MATa/MATa PMR1::HA/PMR1::HA/PMR1::HA PMR1::HA ade2/ade2/ade2/ade2 his3Δ200/his3Δ200/his3Δ200/his3Δ200 leu2-3,112/leu2-3,112/leu2-3,112/leu2-3,112 lys2Δ201/lys2Δ201/ lys2Δ201/lys2Δ201 ura3-52/ura3-52/ura3-52/ura-52*	This work
AA660	*MATα/MATα/MATa/MATa ade2/ade2/ade2/ade2 his3Δ200/his3Δ200/his3Δ200/his3Δ200 leu2-3,112/leu2-3,112/leu2-3,112/leu2-3,112 lys2Δ201/lys2Δ201/lys2Δ201/lys2Δ201 ura3-52/ura3-52/ura3-52*	This work
AA662	*MATα/MATa PMR1::HA/PMR1::HA ade2/ade2 his3Δ200/hisΔ200 leu2-3,112/leu2-3,112 lys2Δ201/ lys2Δ201 ura3-52/ura3-52*	This work
AA680	*MATa sec6-4 ade2 his3Δ200 leu2-3,112 ura3-52*	This work
AA682	*MATα sec6-4 pmr1-1::LEU2 his3Δ200 leu2-3,112 lys2Δ201 ura3-52*	This work
AA688	*MATα sec6-4 pmr1-1::LEU2 leu2-3,112 his3Δ200 ura3-52*	This work
AA691	*MATa sec6-4 pmr1-1::LEU2 ade2 lys2Δ201 leu2-3,112 his3Δ200 ura3-52*	This work
AA696	*MATa sec15-1 pmr1-1::LEU2 lys2Δ201 leu2-3,112 his3Δ200 ura3-52*	This work
AA697	*MATa sec15-1 pmr1-1::LEU2 lys2Δ201 leu2-3,112 his3Δ200 ura3-52*	This work
AA710	*MATa sec19-1 pmr1-1::LEU2 ade2 lys2Δ201 ura3-52 his3Δ200*	This work
AA716	*MATα sec19-1 pmr1-1::LEU2 ade2 lys2Δ201 ura3-52*	This work
AA720	*MATa/MATα sec18-1/sec18-1 +/ ade2 leu2-3,112/leu2-3,112 lys2Δ201/lys2Δ201 ura3-52/ura3-52* (pL161)	This work
AA724	*MATa/MATα sec7-1/sec7-1 ade2/ade2 his3Δ200/his3Δ200 leu2-3,112/leu2-3,112 + /lys2Δ201 ura3-52/ ura3-52* (pL161)	This work
AA728	*MATa/MATα sec6-4/sec6-4 his3Δ200/+ leu2-3,112/leu2-3,112 ura3-52/ura3-52* (pL161)	This work
NY768	*MATα sec1-1 leu2-3,112 ura3-52*	P. Novick (Yale University)
NY770	*MATα sec2-41 leu2-3,112 ura3-52*	P. Novick (Yale University)
NY772	*MATa sec3-2 leu2-3,112 ura3-52*	P. Novick (Yale University)
NY774	*MATa sec4-8 leu2-3,112 ura3-52*	P. Novick (Yale University)
NY776	*MATa sec5-24 leu2-3,112 ura3-52*	P. Novick (Yale University)
NY778	*MATα sec6-4 leu2-3,112 ura3-52*	P. Novick (Yale University)
NY780	*MATα sec8-9 leu2-3,112 ura3-52*	P. Novick (Yale University)
NY782	*MATa sec9-4 leu2-3,112 ura3-52*	P. Novick (Yale University)
NY784	*MATa sec10-2 leu2-3,112 ura3-52*	P. Novick (Yale University)
NY786	*MATa sec15-1 leu2-3,112 ura3-52*	P. Novick (Yale University)
ANY119	*MATα bet2-1 his4-619 ura3-52*	S. Ferro-Novick (Yale University)
AFY93	*MATα mnn1 ura3*	A. Franzusoff (U. of Colorado, Denver)
L2851	*MATα sec53-6 ade2 ura3*	G. Fink
L4648	*MATa sst2::URA3 leu2-3,112 lys2-801 trp1Δ1 ura3-52*	E. Elion (Harvard University)
RSY153	*MATα sec63-1 leu2-3,112 ura3-52*	R. Schekman (U.C. Berkeley)
RSY455	*MATa sec61-3 leu2-3,112 ura3-52 trpl-1 his4 HOL1-1*	R. Schekman (U.C. Berkeley)
RSY530	*MATα sec62 leu2-3,112 ura3-52*	R. Schekman (U.C. Berkeley)

Table 2. Percentage of different markers found in peak PMR1 fractions (fractions 5–7) from the gradient diagrammed in Figure 2

Marker	Percent
PMR1	55.4
KEX2	50.1
GDPase	57.5
PMA1	1.1
NADPH cytochrome c reductase	2.2
α mannosidase	29.7

(Rose *et al.*, 1989); crude anti-SEC7 antisera, 1:250 (Franzusoff *et al.*, 1991a); affinity-purified anti-KEX2, 1:100 (Franzusoff *et al.*, 1991a; Redding *et al.*, 1991). Secondary fluorescent antibodies (Jackson Immunoresearch, West Grove, PA) were diluted as follows: DTAF-conjugated goat anti-mouse immunoglobulin (Ig) (DTAF: 5-[(4,6-dichlorotriazin-2-y)amino]fluorescein), 1:50, labeling bound 12CA5 antibody; Texas Red–conjugated donkey anti-rabbit IgG, 1:200, labeling bound αKAR2, αSEC7, or αKEX2 antibodies. As controls for double-labeling experiments, one or the other primary antibody was excluded from the primary incubation step. Spurious cross reactivity as detected by labeling with the inappropriate fluorescent secondary antibody was never observed. In addition, appropriate labeling of the cognate primary was shown to be unperturbed by the presence or absence of the other primary antibody. Where feasible, deletion strain controls were run (e.g., *kex2Δ*, *PMR1* untagged strains). 4′6-diamidino-2-phenylindole · 2HCl (DAPI) staining, slide preparation, microscopy, and photography were carried out as described (Davis and Fink, 1990). For the analysis of colocalization data, photographic negatives were projected through an enlarger exposing Kodak XAR 5 film for 0.2 s at f16 to give an enlarged light transparent positive. This procedure allowed images to be superimposed for close comparison. The staining of PMR1::HA by indirect immunofluorescence in various *sec* mutants was carried out as described in the legend of Figure 5. For the quantitation of the number of ovoid structures per cell in wild-type and *sec7* strains, at the permissive and restrictive temperature, inclusions > ~1.5 μm were counted on a photographic image of a field and divided by the total number of stained cells to give the average number of inclusions per cell (the number of cells counted >50 for each class).

Subcellular Fractionation

The procedure for subcellular fractionation was based on sedimentation through sucrose density gradients in the presence of $MgCl_2$, developed by Abeijon *et al.* (1989), but contained several modifications. Cells were grown in synthetic complete media (SC) or SC minus uracil (when maintaining URA3-based plasmids) to early logarithmic phase (0.15–0.4 OD_{600} U/ml). Cultures were rapidly chilled on ice, and 300–400 OD_{600} units of cells were harvested by centrifugation at 6000 × *g* for 10 min. All subsequent steps were carried out on ice unless noted otherwise. The cell pellet was resuspended in 30 ml of ice cold 10 mM NaN_3 and centrifuged 5 min at 2000 × *g*. Cells were resuspended in 5 ml of SB buffer [1.4 M sorbitol, 50 mM Tris HCl pH 7.5, 10 mM NaN_3, 40 mM betamercaptoethanol (BME)], 0.5 mM phenylmethylsulfonyl fluoride (PMSF)], sonicated 5 s to disperse clumped cells, and oxalyticase (Enzogenetics, Eugene, OR) was added to 0.1 mg/ml. Cells were converted to spheroplasts for 30 min at 37°C with occasional gentle shaking. The spheroplast suspension was adjusted to 1 mM EDTA, chilled on ice, layered on top of 8 ml of 1.8 M sorbitol, and spheroplasts were pelleted through the sorbitol cushion for 12 min at 450 × *g* (1.7 K rpm in Sorvall RT6000). The supernatant was aspirated, the spheroplast pellet gently loosened with a glass rod and vortexed at low speed. Lysis buffer [20 mM triethanolamine acetate pH 7.2, 12.5% sucrose (w/v), 1 mM EDTA] containing protease inhibitors [0.4 mM PMSF, 0.1 mM L-1-tosylamide-2-phenylethylchloromethyl ketone (TPCK), 25 μM pepstatin A, 1 mM benzamidine HCl, and 1 μg/ml each of leupeptin, antipain, and chymostatin, all purchased from Sigma Chemical, St. Louis, MO] was added to 6 ml. The spheroplast suspension was gently sheared by drawing it in and out of a serological pipette several times, followed by very gentle vortexing, and hand mixing. The lysate was homogenized with 10 strokes of a Wheaton A dounce homogenizer (Wheaton Scientific, Millville, NJ) and then centrifuged 3 min at 450 × *g* to remove unlysed cells, to produce the supernatant (S_{450}) and the pellet (P_{450}). In some cases, the S_{450} was again spun 3 min at 450 × *g* to remove remaining cell clumps and large debris. The resulting pellet fraction was combined with the first and called the P_{450}. One milliliter of the resultant S_{450} (~60 OD_{600} equivalents) was layered onto gradients containing 1-ml steps of 18, 22, 26, 30, 34, 38, 42, 46, 50, and 54% sucrose (wt/wt) in 10 mM *N*-2-hydroxyethylpiperazine-*N*′-2-ethanesulfonic acid (HEPES) pH 7.5, 1 mM $MgCl_2$. Gradients were spun 2.5 h at 38 000 rpm (174 000 × *g*) in a Beckman SW41 rotor (Beckman Instruments, Palo Alto, CA) at 4°C. Gradients were fractionated from top to bottom with a Buchler autodensiflow fractionator (Buchler Instruments, Lenexa, KS) and collected in 16-drop (~660 μl) fractions. The pellet at the bottom of the tube was resuspended in the last fraction. Protease inhibitors were added to the fractions.

Western Immunoblot Analysis of Gradients Fractions

Samples for Western analysis were prepared by taking 40-μl aliquots from each fraction, adjusting them to 1% SDS, 2% BME, 0.15 M Tris HCl pH 6.8, 0.01% bromophenol blue, and then heating them for 5 min at 60°C. Samples were loaded on 10% polyacylamide gels and subjected to SDS-PAGE. Proteins were electrophoretically transferred to nitrocellulose, and blots were cut into horizontal strips centered around the molecular weight of the various antigens. Blocking, antibody and [^{125}I]-Protein A incubations, and quantitation were carried out as described under *Quantitation of Autoradiograms*.

Enzyme Assays

Boc-gln-arg-arg-7 amino 4 methylcoumarin, the substrate for KEX2 assays, was purchased from Peninsula Labs, Belmont, CA. All other reagents were purchased from Sigma Chemical. Typically 20–25 μl of extract were used in all assays. Reactions were carried out in a total volume of 100 μl, except for NADPH cytochrome c reductase assays which were carried out in a volume of 1 ml. Guanosinediphosphatase (GDPase) was assayed according to Abeijon *et al.* (1989). Liberated phosphate was measured with the Fiske Subbarow kit from Sigma Chemical. Nonspecific NDPase plus free P_i were determined using CDP as a nonspecific substrate. These values were subtracted from those obtained with the substrate GDP to give GDPase activity. NADPH cytochrome c reductase was assayed according to Feldman *et al.* (1987); α mannosidase was assayed according to the method of Opheim (1978); latent KEX2 protease activity was assayed according to the method of Cunningham and Wickner (1989); and protein concentration was determined by the Bradford method (1976). Sucrose density was measured with a Bausch and Lomb refractometer (Rochester, NY).

RESULTS

Epitope-Tagged PMR1 Protein for Localization

To follow the PMR1 protein, we constructed a version of the *PMR1* gene (*PMR1::HA*) that encodes a *PMR1* gene product tagged with nine amino acids from the influenza hemagglutinin protein (the HA epitope, Wilson *et al.*, 1984) at its amino terminus. *PMR1::HA* encodes a fusion protein that retains activity as it complements the *pmr1* deletion for growth on low Ca^{2+} media (Figure 1C) and for its sporulation defect. On

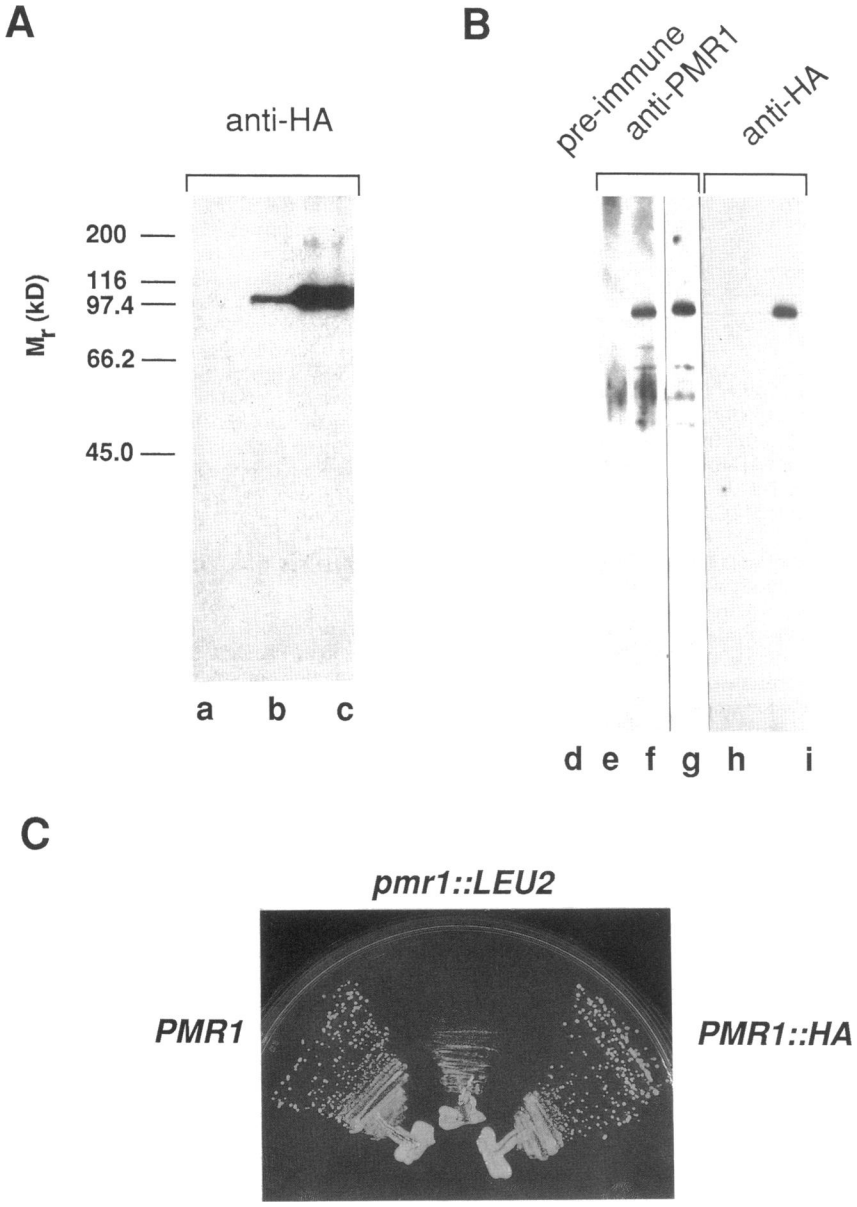

Figure 1. (A) Monoclonal antibody 12CA5 (Field *et al.*, 1988) specifically recognizes a 105-kDa protein corresponding to the *PMR1::HA* gene product. Protein extracts were made from *pmr1* deletion strain AA274 transformed with plasmids pL149 (single copy untagged *PMR1* CEN, lane a), pL149/N13 (single copy *PMR1::HA* CEN, lane b) and pL161 (multiple copy *PMR1::HA* 2μ, lane c). Western blots were probed sequentially with monoclonal antibody 12CA5, rabbit anti-mouse IgG, and [^{125}I]-Protein A. (B) Mouse polyclonal antibodies generated against a TrpE::PMR1 fusion protein (pL144) recognize a band of similar mobility and intensity as that seen by anti-HA monoclonal 12CA5 in Western blots. Lane d: preimmune sera applied to immunoblotted extracts derived from strain AA274(pL129) (strain AA274(pL129) corresponds to AA274 transformed with pL129, a high copy 2μ vector carrying *PMR1*). Lanes e–g: α-PMR1 polyclonal antisera applied to extracts from AA274, AA274(pL129), and AA530 (containing *PMR1::HA* on a multicopy 2μ plasmid), respectively. Lanes h and i: extracts from AA274(pL129) and AA530 probed with monoclonal 12CA5. (C) The *PMR1::HA* allele is functionally competent. The *pmr1* deletion strain AA274 grows poorly on Ca^{2+}-deficient medium, but strains carrying the *PMR1::HA* (AA577) or *PMR1* (AA255) alleles grow equally well.

Western blots, the 12CA5 monoclonal antibody recognizes a distinct protein that has the mobility predicted for PMR1::HA (105 kDa). This band is not present in extracts made from strains lacking *PMR1::HA* and is ~10-fold more abundant in strains containing *PMR1::HA* on a multicopy 2μ plasmid (Figure 1A, lanes a–c). A band of similar mobility and intensity representing the native untagged protein is seen in Western blots with mouse polyclonal antisera generated against a TrpE::PMR1 fusion protein (cf. lanes f and i, Figure 1B). This same band is absent in extracts made from *pmr1* deletion strains and present at similar levels in strains overproducing PMR1 or PMR1::HA on a 2μ plasmid (Figure 1B, lanes e–g). The comparable behavior of native PMR1 and PMR1::HA when visualized with the polyclonal antisera and the functional equivalence of PMR1 and PMR1::HA validate the use of the epitope-tagged gene for localization studies. All of the localization studies described below use the epitope-tagged protein, which will be referred to simply as PMR1, and the 12CA5 monoclonal antibody directed against the HA epitope.

PMR1 Comigrates with Golgi Markers in Subcellular Fractionation

PMR1 was localized by the subcellular fractionation of extracts prepared from gently lysed spheroplasts resolved by velocity sedimentation through sucrose gradients. The various subcellular compartments were identified in gradient fractions by measuring protein or enzymatic markers characteristic for each organelle (see

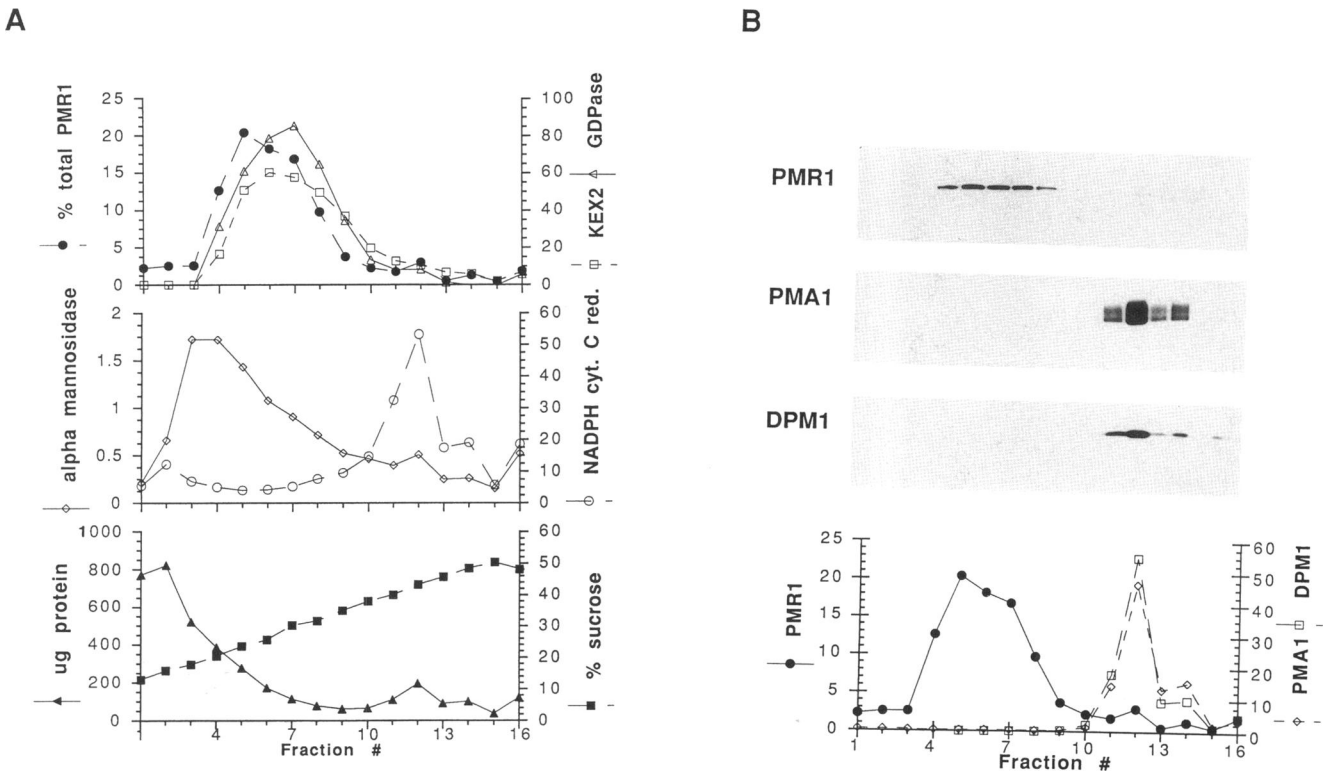

Figure 2. Subcellular distribution of PMR1. (A) PMR1 comigrates with Golgi markers KEX2 and GDPase. The S_{450} prepared from strain AA662 was layered on 18–54% sucrose gradients, and subcellular organelles separated during a 2.5-h spin at 174 000 × *g* as described in MATERIALS AND METHODS. PMR1::HA was detected with the 12CA5 monoclonal (Field *et al.*, 1988) on Western blots. For enzymatic assays, NADPH cytochrome c reductase activity was measured as an ER marker, guanosinediphosphatase (GDPase) and KEX2 protease as Golgi markers, and α mannosidase as the vacuolar marker (see MATERIALS AND METHODS). Fraction 1, top of the gradient; fraction 16, bottom. Units are expressed on a per fraction basis. PMR1 (●) (expressed as percent total of PMR1 antigenic material summed over the whole gradient), GDPase (△) (1 unit = nmole phosphate produced per minute), KEX2 (□) (1 unit = nmole of substrate, BOC-gln-arg-arg-7-amino-4-methylcoumarin, cleaved per hour), NADPH cytochrome c reductase (○) (1 unit = nmole cytochrome C reduced per minute), alpha mannosidase (◇) (1 unit = nmole methylumbelliferyl α-D-mannose cleaved per hour), protein (▲), % sucrose (w/w) (■). (B) PMR1 fractionates away from the plasma membrane marker PMA1 (the plasma membrane H^+-ATPase) and the ER marker DPM1 (dol-P-man-synthase). Aliquots (40 μl) from sucrose density gradient fractions were electrophoretically resolved through 10% SDS-polyacrylamide gels. Proteins were electrophoretically transferred to nitrocellulose and the blots incubated with antibodies and [^{125}I]-Protein A. Blots were exposed to preflashed Kodak XAR 5 film and exposed at −70°C with an intensifying screen. Top: immunoblot analysis of fractions (from the gradient illustrated in Figure 2A); bottom: densitometric scans of autoradiogram exposures with Imagequant software. Quantities are expressed as percent total material. The Y axis on the left corresponds to the scale for PMR1; the Y axis on the right corresponds to the scale for PMA1 and DPM1. PMR1 (●), PMA1 (◇), DPM1 (□). The small amount of PMR1 that does appear in the ER fraction varied from experiment to experiment and probably reflects the mixed nature of this fraction as indicated by the presence of other markers.

Figure 2 legend and MATERIALS AND METHODS). The majority of PMR1 was found in the low-speed supernatant prepared from lysed cells (S_{450}), and most of this material was recovered from the gradient (typically, 73% of PMR1 in the S_{450} was recovered from gradient fractions). The bulk of PMR1 appears to comigrate with the Golgi markers, GDPase (Abeijon *et al.*, 1989) and KEX2 protease (Bowser and Novick, 1991; Cunningham and Wickner, 1989; Redding *et al.*, 1991), and separates from endoplasmic reticulum, plasma membrane, and vacuolar markers (Table 2, Figure 2, A and B, Figure 11). The Western blots in Figure 2B illustrate clearly that the majority of PMR1 is not associated with the plasma membrane or the ER, the two major sites of localization for most known Ca^{2+} pumps in nonmuscle cells of higher metazoans (Carafoli, 1987). PMR1 also separates from the lumenal ER marker, KAR2 (Figure 11), the yeast BiP homolôgue (Rose *et al.*, 1989; Normington *et al.*, 1989). Although PMR1 comigrates roughly with Golgi markers, its peak is slightly displaced from that of KEX2 and GDPase. The overlap with these markers is consistent with a Golgi localization for PMR1, although the altered profiles could reflect a different subcellular distribution.

PMR1 Localizes to a Golgi-like Organelle that Overlaps with but Is Distinct from the SEC7 and KEX2 Compartments

Staining of PMR1 by indirect immunofluorescence reveals a punctate pattern similar to that obtained with proteins thought to be associated with the Golgi (YPT1,

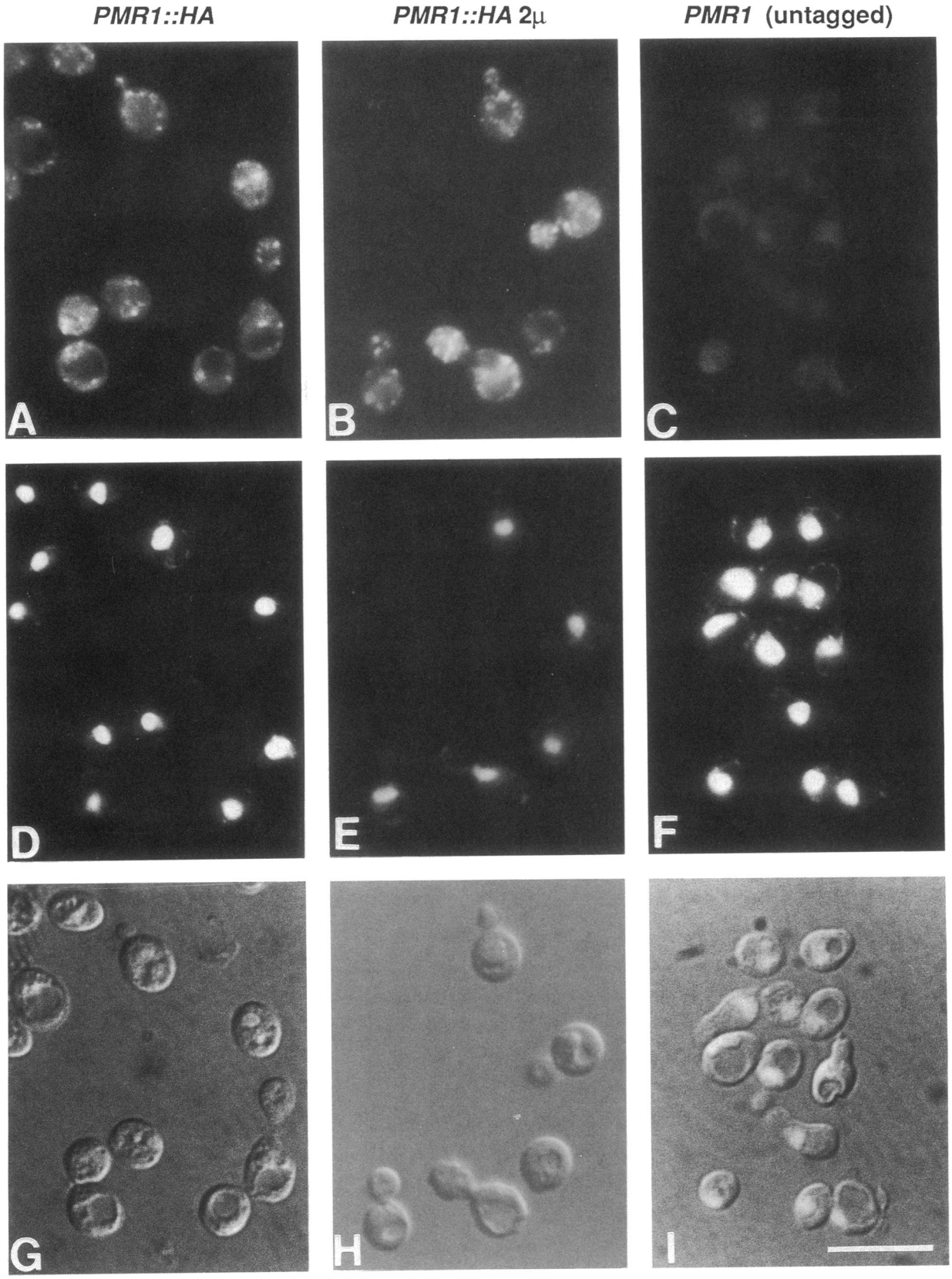
PMR1::HA
PMR1::HA 2μ
PMR1 (untagged)
A
B
C
D
E
F
G
H
I

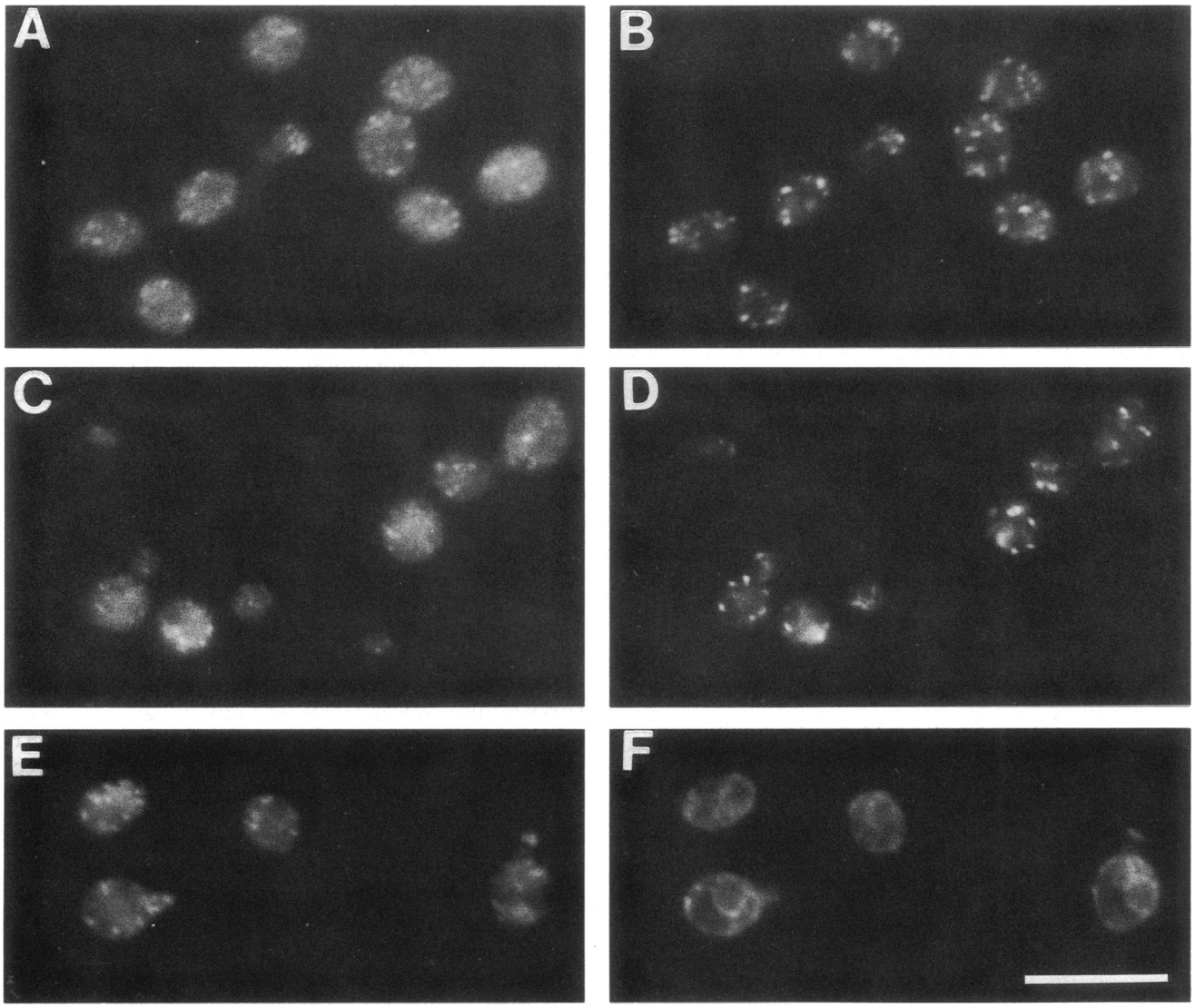

Figure 4. The majority of PMR1 is found in a compartment distinct from compartments containing the Golgi markers SEC7 and KEX2, and the ER marker KAR2. Double-label immunofluorescence was carried out as described in MATERIALS AND METHODS. (A and B) Double-labeling with PMR1 and SEC7, respectively, in strain AA662. (C and D) Double-labeling with PMR1 and KEX2, respectively, in strain AA662 transformed with *KEX2* containing plasmid, YCp-KX212. (E and F) Double-labeling with PMR1 and KAR2, respectively, in strain AA530 (bar = 10 μm).

Segev *et al.*, 1988; KEX2 and SEC7, Franzusoff *et al.*, 1991a; Redding *et al.*, 1991; SEC14, Cleves *et al.*, 1991) or post-Golgi vesicles (Sec4p, Goud *et al.*, 1988). Although the punctate pattern of PMR1 could be observed in cells containing *PMR1::HA* on a CEN-based vector, the clearest visualization was obtained in tetraploid cells containing four copies of the integrated *PMR1::HA* allele (Figure 3A) or multiple copies of *PMR1::HA* on a 2 μ plasmid (Figure 3B). Punctate staining could also be seen in diploids carrying two copies of the integrated gene (Figure 4A). Although higher gene dosage intensifies fluorescent staining and hence the resolution between

Figure 3. Indirect immunofluorescent staining of PMR1 gives a punctate staining pattern. Immunofluorescence was performed as described in MATERIALS AND METHODS with anti-HA monoclonal 12CA5 as a primary antibody and DTAF-labeled goat anti-mouse IgG to visualize sites of primary antibody binding. (A) tetraploid strain, AA654, harboring four integrated copies of epitope-tagged *PMR1::HA*. (B) Strain AA530 containing *PMR1::HA* on a multicopy 2μ plasmid. (C) An untagged *PMR1* strain, AA660, as the negative control for antibody specificity. (D–F) Corresponding DAPI stained nuclei of these cells. (G–I) Respective Nomarski optics with DAPI staining superimposed. The yeast vacuole is the large indentation seen in Nomarski images (bar = 10 μm).

Table 3. Colocalization of PMR1 with SEC7 and KEX2

	Antigen	Colocalize	Fail to colocalize	% Colocalization
Experiment 1	PMR1	55	260	17
AA662	SEC7	55	321	15
Experiment 2	PMR1	61	163	27
AA662 (YCp-KX212)	KEX2	61	172	26

Values refer (from left to right) to the number of punctate staining dots which colocalize, the number of dots which fail to colocalize, and the percent colocalization with respect to a given antigen.

individual puncta, the general staining pattern remained qualitatively similar in all constructs. We typically observed between 4 and 12 dots per cell in a given focal plane, with some puncta appearing larger than others. This staining is specific for PMR1::HA as only faint homogeneous staining of the internal contents of the cell was observed when the untagged control strain was labeled (Figure 3C). The profile of DAPI staining (Figure 3, D and E) shows that PMR1 is neither nuclear, nor perinuclear, and is not associated with mitochondria. Comparison of PMR1 distribution with Nomarski images of whole cells (Figure 3, G and H) demonstrates that PMR1 is neither plasma membrane associated nor vacuolar.

The distribution of PMR1 was compared with that of the Golgi markers, KEX2 and SEC7 (Franzusoff *et al.*, 1991a; Redding *et al.*, 1991), and the lumenal ER marker KAR2 (Rose *et al.*, 1989) by double-labeling immunofluorescence (see Figure 4 and Table 3). Although both PMR1 and SEC7 give rise to punctate staining patterns with similar numbers of puncta per cell, the two arrays are largely not congruent (Figure 4, A and B). The staining associated with SEC7 colocalizes with PMR1 only 15% of the time (Table 3, experiment 1), whereas only 17% of the PMR1 associated dots colocalize with SEC7. In fact, PMR1 and SEC7 often appear to be juxtaposed but nonoverlapping. PMR1 and KEX2 demonstrate a somewhat greater degree of colocalization (27%) than the overlap seen with SEC7 (Figure 4, C and D) though, again the majority of PMR1 staining dots do not superimpose with the KEX2 pattern (Table 3, Experiment 2). Because SEC7 and KEX2, which colocalize in the Golgi complex in yeast (Franzusoff *et al.*, 1991a), fail to show substantial overlap with PMR1, the majority of PMR1 may be sequestered in a subcompartment of the Golgi or may reside in pre- or post-Golgi compartments. The KAR2 and PMR1 patterns are completely distinct (Figure 4, E and F), confirming the results of subcellular fractionation experiments. The regions of intense PMR1 staining lie in the interstitial spaces between the perinuclear and cortical membranes of the ER delineated by KAR2 staining (Rose *et al.*, 1989).

PMR1 Has an Altered Distribution in a sec7 Mutant

The distribution of PMR1 was determined in three representative *sec* mutants, *sec7*, *sec6*, and *sec18*. *sec7* strains have been shown by electron microscopy to accumulate aberrant, distended Golgi-like cisternae at 37°C under low glucose conditions (Esmon *et al.*, 1981; Novick *et al.*, 1980; Novick *et al.*, 1981). In *sec7* cells grown at 37°C under low glucose, PMR1 is localized in enlarged, brightly staining ovoid structures (Figure 5), whereas at the permissive temperature (24°C) the staining was more similar to the punctate pattern found in wild-type cells. Although large staining puncta are seen on occasion in wild type or the *sec7* mutant under permissive conditions, the proportion of these ovoid structures is greater in *sec7* mutants at 37°C. The average number of inclusions per cell for *sec7* at the restrictive temperature, *sec7* at the permissive temperature and wild type were 1.2, 0.29, and 0.36, respectively. The PMR1 staining pattern resembles that of YPT1, a Golgi-associated antigen, when stained by indirect immunofluorescence in a *sec7* mutant (Segev *et al.*, 1988). The lumenal ER marker, KAR2, gives typical perinuclear ER staining in a *sec7* mutant, indicating that *sec7* does not lead to general disarray of internal compartments.

The distribution of PMR1 is not altered significantly in either *sec18* or *sec6* mutants. At the nonpermissive temperature, *sec6* mutants accumulate large numbers of post-Golgi secretory vesicles (Esmon *et al.*, 1981; Novick *et al.*, 1980) that can be visualized by indirect immunofluorescence with anti-Sec4p antibody (Goud *et al.*, 1988). Unlike the staining of Sec4p in *sec6* strains, PMR1 staining in *sec6* remains unchanged, a result that suggests that PMR1 is not a component of post-Golgi secretory vesicles (Figure 5). The punctate staining pattern of PMR1 persists in *sec18* strains, a mutant that accumulates ER and small vesicles (Novick *et al.*, 1980; Kaiser and Schekman, 1990), but the staining is fainter (Figure 5). Failure to find distinct staining of newly synthesized PMR1 in the ER of *sec18* could reflect a low rate of PMR1 synthesis or rapid degradation of the protein when abnormally retained in the ER membrane.

pmr1 Strains Are Defective in the Addition of Outer-Chain Mannose Residues

Invertase isolated from a *pmr1* strain migrates as a relatively discrete band with a mobility intermediate between that of the core-glycosylated forms produced in a *sec18* mutant (Esmon *et al.*, 1981) and that of the heterogeneous highly glycosylated forms synthesized in wild-type strains (Figures 6A and 7, cf. lanes 1, 7, and 10). The *pmr1 sec18* double mutant exhibits only the core glycosylation pattern associated with the *sec18* single mutant, showing that the *sec18* block precedes the *pmr1* glycosylation defect (Figure 6A). In similar double mutant analyses, the *pmr1* truncated glycosylation pattern prevails over the pattern of underglycosylation observed in the ER/Golgi-blocked *ypt1-1* (cs) mutant (Se-

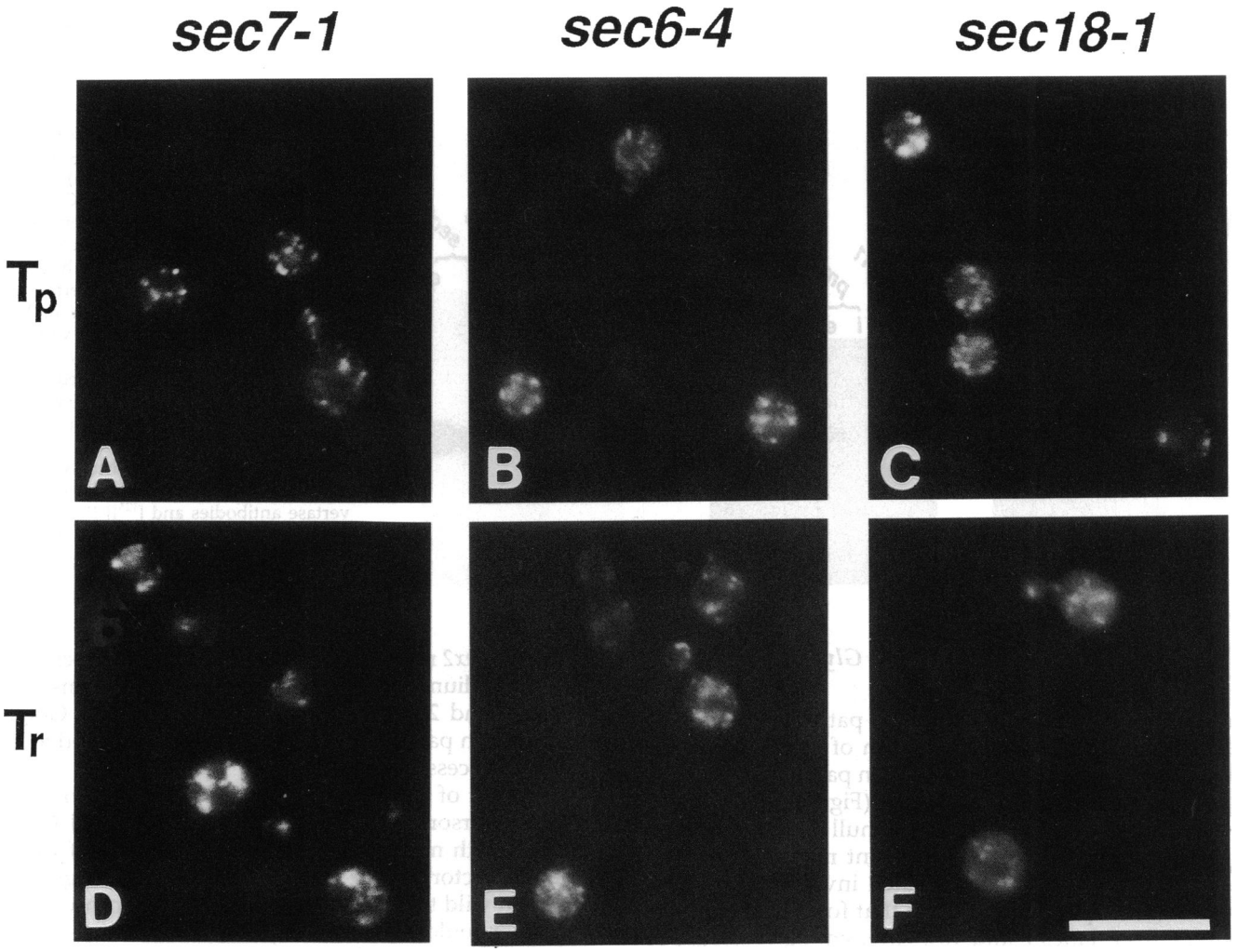

Figure 5. Staining by indirect immunofluorescence of PMR1::HA in a *sec7-1* mutant reveals an aberrant Golgi-like structure. Strains AA724 (*sec7-1*), AA728 (*sec6-4*), and AA720 (*sec18-1*) carrying *PMR1::HA* 2μ were grown to logarithmic phase in 2% glucose SC minus uracil media at 23°C, (the permissive temperature), washed, and resuspended in 0.1% glucose SC minus uracil media and incubated at the permissive or restrictive temperature for various times. AA724 was temperature shifted to 37°C for 2 h, AA728 was shifted to 36°C for 2 h, and AA720 was shifted to 30°C for 1 h. Cells were then fixed, permeabilized, incubated with anti-HA antibody, and stained with DTAF-conjugated goat anti-mouse IgG. The top row shows cultures grown at the permissive temperature (T_p); the bottom row shows cultures grown at the restrictive temperature (T_r). (A) *sec7-1*, 23°C; (D) *sec7-1*, 37°C; (B) *sec6-4*, 23°C; (E) *sec6-4*, 36°C; (C) *sec18-1*, 23°C; (F) *sec18-1*, 30°C (bar = 10 μm).

gev *et al.*, 1988) or the heterogeneous pattern seen in the post-Golgi-blocked *sec6* mutant (Esmon *et al.*, 1981) (see Figure 6, B and C). These epistatic relationships enable us to assign the glycosylation defect of *pmr1* to a segment of the secretory pathway between the ER and the Golgi.

The nature of the glycosylation defect in *pmr1* became clearer when we analyzed the mannose linkages on secreted invertase with antibodies specific to α1,6 and α1,3 mannose linkages, as signatures of early and late Golgi processing steps, respectively (Franzusoff and Schekman, 1989). Because virtually all the periplasmic invertase secreted from *pmr1* strains (Figure 7, lanes 7–9) receives both α1,6 (99%) and α1,3 mannose linkages (96%), the truncated glycosylation pattern is likely to be a consequence of reduced outer-chain addition; within the total population of invertase, nearly every molecule contains both linkages, but the extent of either α1,6 or α1,3 linkages or both is likely to be diminished. Corrorboratively, secreted pro-alpha factor immunoprecipitated from *pmr1* strains similarly receives both α1,6 and α1,3 mannose linkages. The failure of *pmr1* strains to elongate outer chains does not appear to be due to more rapid secretion in the mutant strains because pulse chase experiments indicate that the time at which 50% of the pulse-labeled invertase is externalized is approximately the same for *pmr1* and wild-type strains (4 and 5 min, respectively).

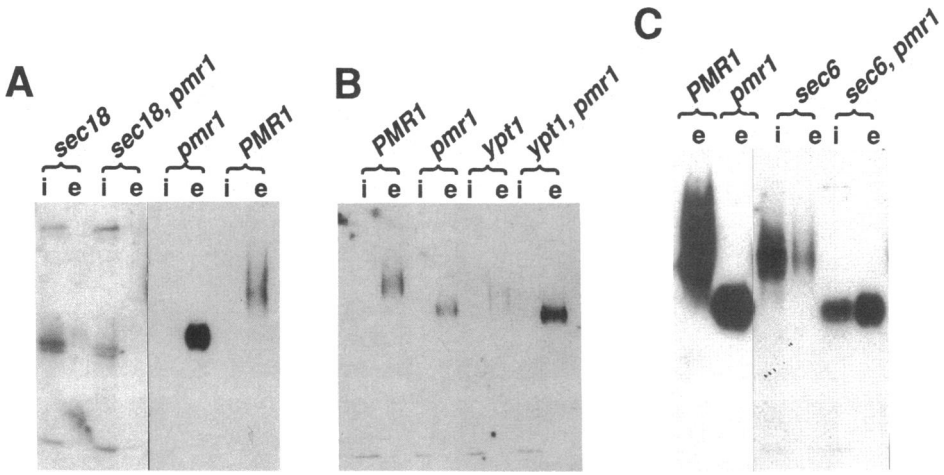

Figure 6. Analysis of internal and external invertase from *pmr1* and *pmr1 sec* double mutants. Strains AA255, AA274, AA401, AA402, AA460, AA470, AA680, and AA682 were grown to logarithmic phase in YP 5% glucose supplemented with 0.5 mM $CaCl_2$ at the permissive temperature [*sec18* (A), 22°C; *ypt1-1* (B), 30°C; *sec6* (C) 22°C], preshifted to the nonpermissive temperature for various amounts of time (*sec18*, 36°C, 0.75 h; *ypt1-1*, 14°C, 3 h; *sec6*, 34°C, 3 h), and induced for invertase at the nonpermissive temperature in YP 0.1% glucose 0.5 mM $CaCl_2$ for various amounts of time (*sec18*, 2 h; *ypt1-1*, 12 h; *sec6*, 2 h). Cells were harvested, converted to spheroplasts, and separated into periplasmic (e) or internal (i) fractions. Extracts were resolved by SDS-7.5% PAGE and subjected to Western analysis applying sequentially anti-invertase antibodies and [^{125}I]-Protein A. Immunoblots were exposed to Kodak XAR 5 film at −70°C with an intensifying screen.

Calcium Partially Suppresses the Glycosylation Defect of pmr1

In *pmr1* strains, the glycosylation pattern of invertase is dependent on the concentration of Ca^{2+} in the medium. In low Ca^{2+}, the glycosylation pattern is truncated and discrete relative to wild type (Figure 8, cf. lanes 3 and 9). However, when the *pmr1* null mutant is grown in high external Ca^{2+}, the apparent molecular weight and heterogeneity of glycosylated invertase increases, resulting in a pattern more like that found in wild type (Figure 8, cf. lanes 7 and 13). After endoglycosidase H treatment, all these forms of invertase migrate more rapidly near the position of the unglycosylated form, showing that glycosylation and not other processing events cause the mobility shift. That Ca^{2+} itself partially restores glycosylation to *pmr1* mutants implicates a role for Ca^{2+} in a post-ER event.

pmr1 Mutants Secrete Unprocessed α Factor and Have a Slight Mating Defect

MATα pmr1 strains secrete multiple forms of unprocessed α factor (Figure 9A). α Factor, a tridecapeptide, is synthesized as a polyprotein containing four repeats of the α-factor peptide attached to an amino terminal glycosylated leader that is cleaved in several processing steps. This processing requires KEX2, an endoprotease that cleaves the polyprotein into discrete peptides in a late Golgi compartment, STE13, a diaminopeptidylpeptidase that removes the N-terminal spacer amino acids, and KEX1, which removes C-terminal amino acids to give the mature secreted 13-amino acid peptide (for review, see Fuller *et al.*, 1988). *pmr1* strains secrete a high-molecular-weight, highly glycosylated form of α-factor precursor and little mature α factor, a profile resembling that of the *kex2* mutant (Julius *et al.*, 1984). Also secreted into the medium is an unidentified ladder of forms between 18 and 28 kDa that may represent early Golgi glycosylation patterns or partial cleavage intermediates in KEX2 processing.

The effect of Ca^{2+} in suppressing the secretion of α factor precursors is striking. Addition of 10 mM Ca^{2+} to the growth medium results in the secretion of fully mature α factor, giving *pmr1-1* a profile indistinguishable from wild type (Figure 9A). The partial processing of α factor could be the consequence of defective KEX2 activity, a known Ca^{2+}-dependent protease (Fuller *et al.*, 1989) or result from the missorting of pro-α-factor, or pro-α-factor–processing enzymes.

The halo bioassay for α-factor–induced growth arrest also confirms that *pmr1* strains produce ~10-fold less α factor than wild type in low Ca^{2+} medium. The addition of 10 mM $CaCl_2$ to the growth medium restores the production of wild-type levels of biologically active α factor (Figure 9B). Consistent with a defect in pheromone production, both *MATapmr1* and *MATαpmr1* strains exhibit weak unilateral mating defects in quantitative mating experiments (Table 4).

Localization of Carboxypeptidase Y and Other Organellar Markers is Relatively Unaffected in pmr1

We examined the trafficking of the vacuolar protein carboxypeptidase Y (CPY) in a *pmr1* mutant, a protein that is missorted in various *vps* and *pep* mutants (see Klionsky *et al.*, 1990 for review). Little CPY is secreted into the medium in *pmr1* strains. The majority of CPY reaches its destination in the vacuole where it is proteolytically matured (mCPY) (Haslik and Tanner, 1978).

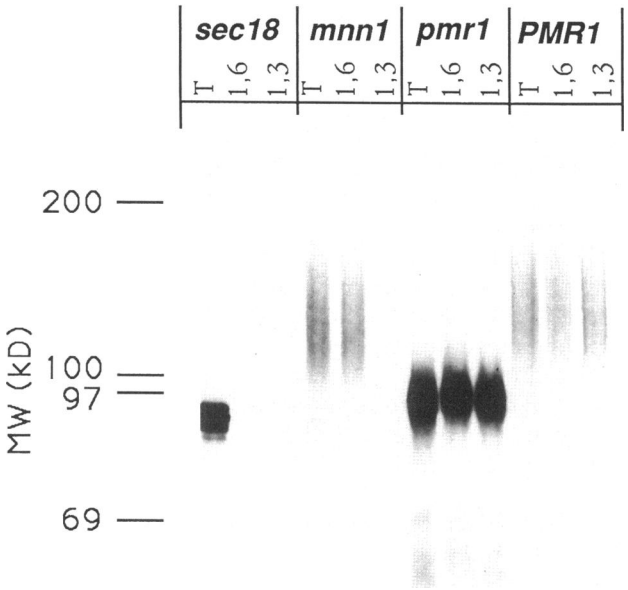

Figure 7. Periplasmic invertase secreted from a *pmr1* background acquires both α1,6 and α1,3 mannose linkages. *pmr1* (AA274) and *PMR1* (AA255) were grown to logarithmic phase in low-sulfate medium, derepressed for invertase synthesis, and pulse labeled with Tran^{35}S-label for 30 min at 30°C. *sec18-1* (AA460) was grown to logarithmic phase at 22°C, derepressed for invertase, shifted to 36°C for 15 min, and pulse labeled at 36°C for 30 min. *mnn1* (AFY93) was grown to log phase, derepressed, and pulse labeled for 45 min at 22°C. AA274 and AA255 cells were converted to spheroplasts and secreted periplasmic invertase was subsequently immunoprecipitated under denaturing conditions. Total invertase from AA460 and AFY93 were prepared by glass bead lysis and immunoprecipitated. In the second round of immunoprecipitation equal amounts of immunoprecipitated invertase were solubilized and incubated with anti-invertase (T), anti-α1,6 mannose (1,6), or anti-α1,3 mannose (1,3) antibodies. Core-glycosylated invertase accumulated in *sec18* fails to receive Golgi carbohydrates and is immunoprecipitated only by anti-invertase antibody. Invertase accumulated in *mnn1*, which is deficient in the α1,3 mannosyl transferase, (Nakajima and Ballou, 1975) is not immunoprecipitated by anti-α1,3 antisera. Wild type receives both linkages.

A small amount (6.7% of the total CPY) of the Golgi intermediate p2 form fails to target to the vacuole and is secreted into the medium in *pmr1* strains (Figure 10). This phenotype is not simply the result of cell lysis because the mature form of vacuolar carboxypeptidase Y is not found in the medium. The p2 form, in addition, has a slightly increased mobility relative to wild type. Both of these phenotypes are reversed by the addition of 10 mM $CaCl_2$ to the medium. The amount of p2 CPY secreted from *pmr1* grown in high Ca^{2+} or from wild type is ~1% or less of the total. By comparison with the dramatic effects of *pmr1* on α-factor processing and invertase glycosylation, the effects of *pmr1* on vacuolar sorting are minor and certainly not of the same magnitude as the vacuolar defects observed in *pep* and *vps* mutants (Klionsky *et al.*, 1990).

We also examined the effect of the *pmr1* mutation on the intracellular distribution of various organellar markers. The fractionation profile of markers for the ER, vacuole, Golgi apparatus, and plasma membrane appears relatively normal in extracts prepared from a *pmr1* mutant (Figure 11). The most notable difference is a threefold reduction in KEX2 specific activity and a threefold increase of vacuolar α mannosidase specific activity in fractionated extracts prepared from *pmr1* (Table 5). Neither the fractionation of the lumenal ER marker, KAR2 (Figure 11), nor its intracellular location as visualized by indirect immunofluorescence appear obviously changed by mutations in *pmr1* (Figure 12). Similarly, the indirect immunofluorescence staining pattern of the Golgi marker, SEC7, appears unperturbed in *pmr1* strains (Figure 12).

pmr1 Deletion Suppresses Various sec *Mutants Blocked in ER/Golgi and Post-Golgi Transport*

The *pmr1* null mutant suppresses a cold-sensitive growth lesion in YPT1 (Rudolph *et al.*, 1989), a GTP binding protein localized to the Golgi (Segev *et al.*, 1988) whose loss of function leads to a block in ER to Golgi transport (Bacon *et al.*, 1989; Baker *et al.*, 1990). We found that the temperature sensitivity of several other *sec* mutants is also suppressed in a *pmr1* background.

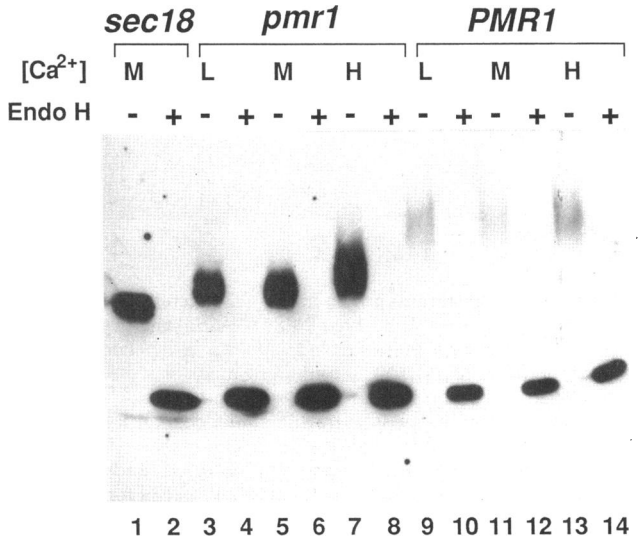

Figure 8. *pmr1* strains secrete invertase with a truncated glycosylation pattern that is partially Ca^{2+} remedial. AA274 (*pmr1*) and AA255 (*PMR1*) cultures were grown to log phase in 5% glucose Ca^{2+}-free synthetic media supplemented with 10 mM (H) or 0.2 mM (M) $CaCl_2$, or unsupplemented (L). Cells (5 OD_{600} Units) were pelleted, washed, and resuspended in the same media containing 0.1% glucose and induced for invertase synthesis for 3 h. Cells were converted to spheroplasts to release secreted periplasmic invertase and extracts were treated with (+) and without (−) endoglycosidase H. Samples were heated in Laemmli's sample buffer and resolved by 7.5% SDS-PAGE. Proteins were transferred to nitrocellulose, and the blot was probed sequentially with anti-invertase antibodies and [^{125}I]-Protein A. The filter was exposed to preflashed Kodak XAR film at −70°C with an intensifying screen. Lane 1, unsecreted core-glycosylated forms of invertase accumulated internally in a *sec18* mutant strain at the nonpermissive temperature for reference.

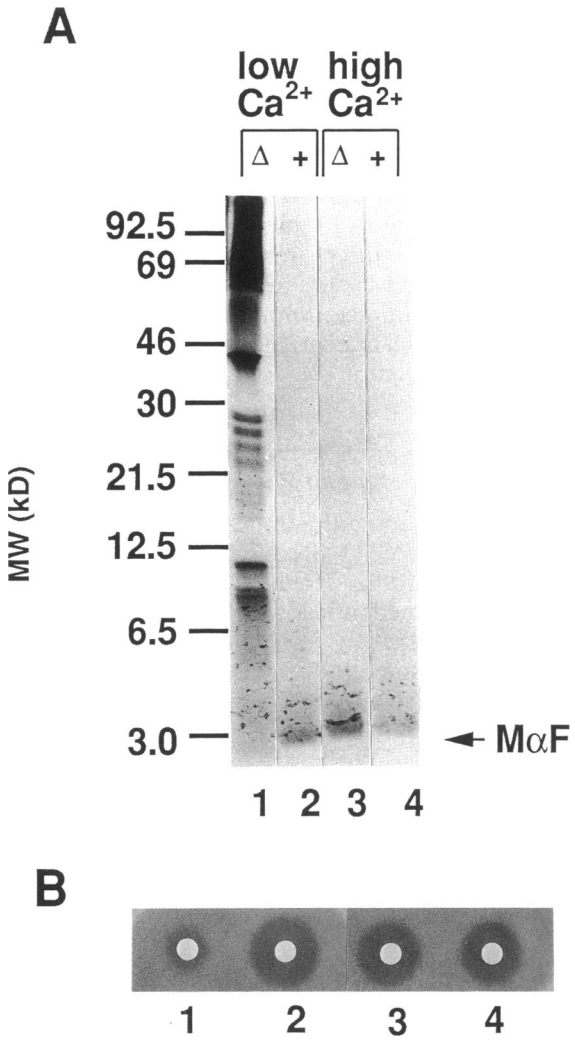

Figure 9. (A) *pmr1* strains grown in low Ca^{2+} secrete multiple forms of unprocessed α factor. Wild-type *PMR1* (AA255) and *pmr1* (AA274) strains were grown and pulse-labeled with tran^{35}S-label in either high (10 mM) or low (200 μM) $CaCl_2$-containing media. Labeled cells were separated into cell and medium fractions, and α factor was immunoprecipitated from the medium fraction under denaturing conditions. Samples were resolved by SDS-PAGE in 17% polyacrylamide gels. Gels were fixed, prepared for fluorography, dried, and exposed to preflashed Kodak XAR film at −70°C. Lane 1, profile of forms secreted from *pmr1* strains in low Ca^{2+}, including highly glycosylated pro-α factor and the ladder of forms between 18 and 28 kDa. Lane 3 demonstrates that the secretion of α factor precursors is abolished in high Ca^{2+}. *MAT*α *PMR1* (+), *MAT*α*pmr1* (Δ). Mature α factor is designated MαF. (B) Halo bioassay for α-factor–induced growth arrest. Concentrated culture supernatants from strains AA274 and AA255 grown in low Ca^{2+} (1 and 2, respectively) or high Ca^{2+} media (3 and 4, respectively) were spotted onto filter disks and placed on a *sst2* lawn (L4648). The difference in halo diameter between sample 1 (culture supernatant from a *pmr1* strain grown in low Ca^{2+} media) and the others represents ~10-fold reduction in α-factor concentration. Halo assays were performed according to Elion and Fink (1990).

Suppression was analyzed first in a set of crosses between a strain carrying a *LEU2* marked *pmr1* deletion and various secretory mutants. These mutants included those that block translocation into or function within the ER, transport from the ER to the Golgi apparatus, traffic through the Golgi complex, and vesicular transport from the Golgi to the plasma membrane (see Table 6) (Novick *et al.*, 1980; Deshaies and Schekman, 1987; Newman and Ferro-Novick, 1987; Schmitt *et al.*, 1988; Segev *et al.*, 1988).

In crosses where *pmr1* suppressed the temperature-sensitive lethality of *sec* mutants, double mutant *pmr1-1::LEU2 sec* ascospores grew, and single *sec* mutant ascospores did not. From the analysis of crosses between nonisogenic strains we found that *sec6-4* and *sec15-1*, restricted in post-Golgi transport, and *sec19-1*, blocked at several steps, were suppressed. To check this result, we constructed isogenic *PMR1 sec* and *pmr1 sec* double mutants by introducing *PMR1* on a CEN vector into the *sec pmr1* background. In agreement with the crossing results the isogenic strains showed suppression of *sec19-1*, *sec6-4*, and weakly *sec15-1* (see Figure 13A, summarized in Table 6). Typically suppression was confined to a narrow temperature range. For instance, *pmr1 sec19* double mutants grow well at 36°C but not at 37°C. Some of these *sec* mutants demonstrated Ca^{2+}-related phenotypes. For example, the *sec19* single mutant is suppressed by the addition of 10 mM $CaCl_2$ to YPD plates, whereas high Ca^{2+} reverses the *pmr1*-dependent suppression in the *pmr1 sec19* double mutant (Table 7). Moreover, *ypt1-1* (cs) partially suppresses the EGTA-sensitive growth defect of *pmr1* strains, an example of cosuppression (Table 7).

PMR1 Overexpression Intensifies the Temperature-Sensitive Growth Defect of Various sec *Mutants*

The effect of overexpressing *PMR1* on the growth phenotype of various *sec* mutants was analyzed by transformation of the *sec* mutants shown in Table 6 with a high copy 2μ plasmid containing *PMR1* under the control of its own promoter (pL129). The temperature-sensitive growth defect of several *sec* mutants was enhanced by *PMR1* overexpression; the presence of the *PMR1* 2μ plasmid narrowed the temperature range at which a particular *sec* mutant could grow. The controls were *sec* strains having *PMR1* on a single copy CEN vector (pL149) and a high copy YEp24 vector without the *PMR1* insert. No significant effect was seen in the growth phenotype of wild-type strains overexpressing *PMR1* on a 2μ plasmid.

The synthetic lethality caused by overexpression of *PMR1* in *sec* mutants is most obvious in *sec21-1* and *ypt1-1*, blocked in ER/Golgi transport and *sec9-1* and *sec10-4*, restricted in post-Golgi transport (Novick *et al.*, 1980; Esmon *et al.*, 1981; Schmitt *et al.*, 1988; Segev *et al.*, 1988). Figure 13B illustrates that *sec21-1* strains bearing *PMR1* 2μ grow well at 24°C but fail to grow at 32°C, whereas the same strain harboring a YEp24 control plasmid grows well at both temperatures. In addition, a number of *sec* mutants, including *sec13-1*, and

sec23-1 in the ER/Golgi class, *sec1-1*, *sec2-41*, *sec6-4*, and *sec15-1* in the post-Golgi class, and *sec19-1*, are significantly, though less strongly affected (Table 6).

DISCUSSION

Mutant strains lacking PMR1, a presumed Ca^{2+} pump, manifest pleiotropic secretory defects. These defects are probably a direct consequence of a failure to deposit Ca^{2+} within the Golgi lumen, because PMR1 localizes to a Golgi-like organelle by subcellular fractionation and indirect immunofluorescence. Many of these disturbances are reversed by the addition of millimolar levels of extracellular Ca^{2+}, suggesting that loss of *pmr1* function leads to defects in Ca^{2+}-dependent activities. Because most metazoan Ca^{2+} pumps have been assigned to the sarco/endoplasmic reticulum or the plasma membrane (Carafoli, 1987), this represents an unusual location for a Ca^{2+} pump.

The compartment in which PMR1 resides is termed "Golgi-like" because its punctate staining in immunofluorescence experiments resembles the pattern seen with other yeast Golgi-associated antigens (Figures 3 and 4). However, the PMR1 pattern is novel in that it only partly overlaps that of known Golgi markers, KEX2 and SEC7 (26% and 17% colocalization, respectively). SEC7 colocalizes with KEX2 at a higher frequency (58%), although these proteins are clearly not completely congruent (Franzusoff *et al.*, 1991a). The partial overlap of KEX2 and SEC7 has been attributed to localization of these proteins to different subcompartments within the Golgi (Franzusoff *et al.*, 1991a). KEX2 is thought to occupy a late Golgi subcompartment, whereas SEC7 may be associated with several Golgi subcompartments (Franzusoff and Schekman, 1989; Franzusoff *et al.*, 1991a,b). Although PMR1 partially overlaps these markers, the majority of PMR1 may be in yet a third subcompartment. In this regard it may be important that nonoverlapping puncta of SEC7 and PMR1 are often seen in close juxtaposition. That the distended Golgi-like inclusions formed in *sec7-1* mutant strains (Novick *et al.*, 1980; Esmon *et al.*, 1981; Segev *et al.*, 1988) are visualized by indirect immunofluorescence staining of PMR1 places PMR1 in the secretory pathway and is consistent with a Golgi localization (Figure 5).

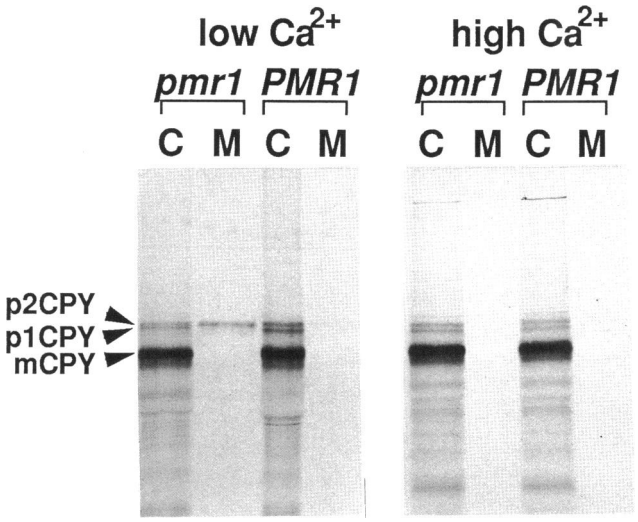

Figure 10. *pmr1* strains missort small amounts (6.7% of the total CPY) of the vacuole bound p2 form of carboxypeptidase Y (p2CPY) into the medium fraction. Wild-type *PMR1* (AA255) and *pmr1* (AA274) strains were grown and pulse-labeled with tran^{35}S-label in either high (10 mM) or low (200 μM) $CaCl_2$. Labeled cells were separated into cell and medium fractions, and CPY was immunoprecipitated from both fractions under denaturing conditions. Immunoprecipitated samples were resolved by SDS-PAGE through 9.0% polyacrylamide. Gels were fixed, prepared for fluorography, dried, and exposed to preflashed Kodak XAR 5 film at −70°C. p1CPY is the core-glycosylated ER form, p2CPY is the Golgi-modified form, and mCPY is the mature vacuolar form.

Our subcellular fractionation experiments also support a Golgi-like distribution for PMR1 (Figure 2). PMR1 fractionates away from endoplasmic reticulum and plasma membrane markers and largely comigrates with the Golgi markers, GDPase, and KEX2 protease (Abeijon *et al.*, 1989; Cunningham and Wickner, 1989; Bowser and Novick, 1991; Redding *et al.*, 1991). However, PMR1 does not strictly follow these markers because the profile of PMR1 in peak fractions and shoulders is often displaced from that of other Golgi markers. This dissimilarity could reflect a different subcompartmental distribution within the Golgi complex, or alternatively represent the profile of a distinct comigrating organelle.

The localization of PMR1 to the Golgi has some ambiguity because the structure of the yeast Golgi complex has not been elucidated. Ultrastructural examination of

Table 4. *pmr1* strains exhibit a weak unilateral mating defect

Cross	Relevant genotype	Diploids/total	% Diploid formation
AA288 × AA280	*MATa PMR1* × *MATα PMR1*	328/565	58
AA300 × AA277	*MATa pmr1* × *MATα PMR1*	127/349	36
AA288 × AA274	*MATa PMR1* × *MATα pmr1*	106/392	27
AA300 × AA298	*MATa pmr1* × *MATα pmr1*	230/1450	16

Quantitative matings were carried out according to Elion *et al.* (1990).

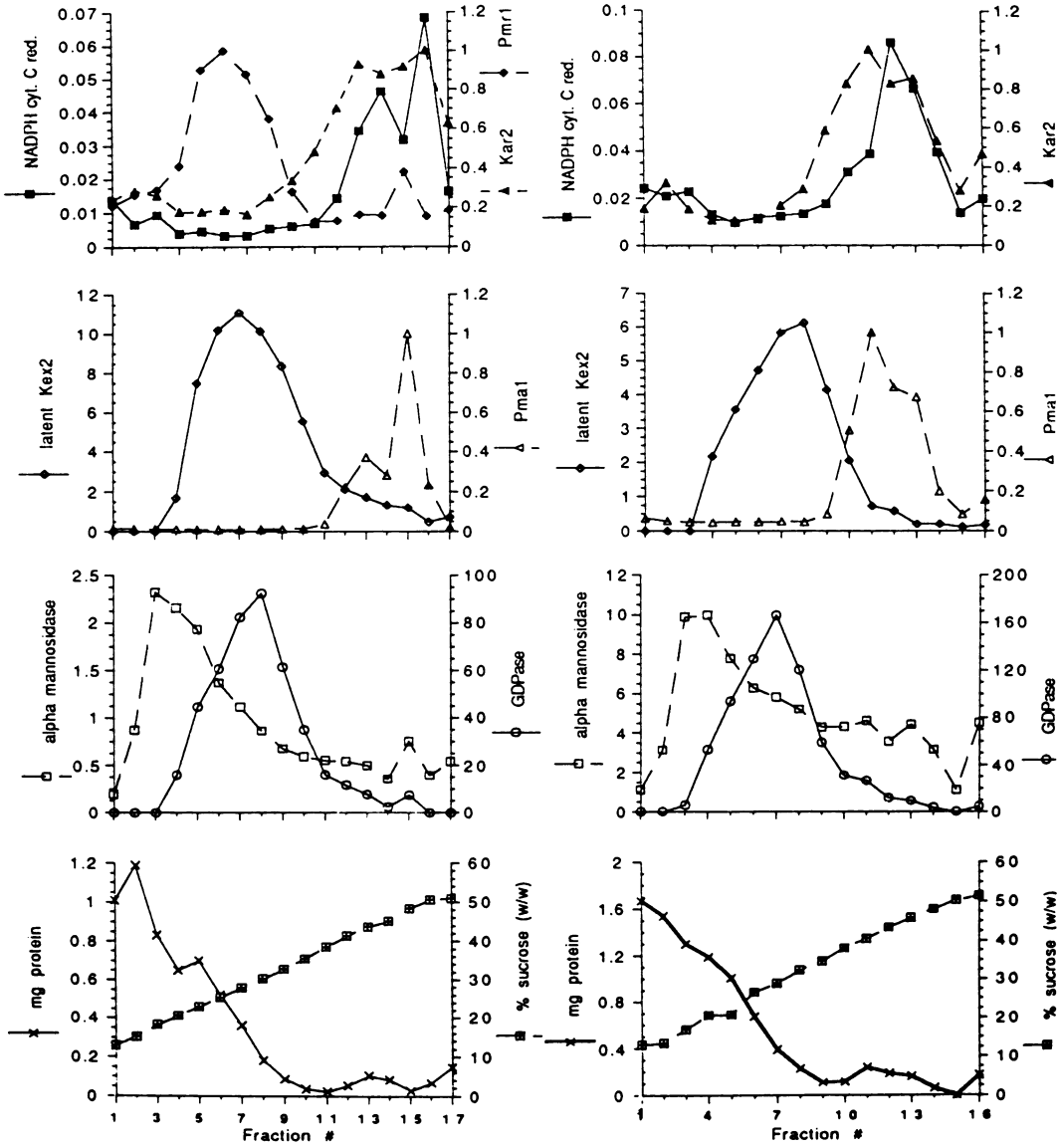

Figure 11. Subcellular fractionation of the S_{450} from *PMR1* (left) and *pmr1* strains (right). The S_{450}s prepared from AA662 (*PMR1::HA*) and AA522 (*pmr1*) were layered on 18–54% sucrose gradients, centrifuged, fractionated, and enzyme markers were assayed as described in the MATERIALS AND METHODS. PMR1 (◆) (expressed as percent maximum PMR1::HA antigenic material), KAR2 (▲) (expressed as percent maximum KAR2 antigenic material), NADPH cytochrome c reductase (■), KEX2 (◇), PMA1 (△) (expressed as percent maximum PMA1 antigenic material), GDPase (○), α mannosidase (□), protein (×), % sucrose (wt/wt) ⊞.

wild-type yeast cells has only recently produced pictures of a morphologically identifiable Golgi apparatus containing cisternae that resemble those found in higher eukaryotes (Preuss *et al.*, 1992). Staining of presumed Golgi antigens by indirect immunofluorescence reveals a punctate staining pattern that is dispersed, heterogeneous, and morphologically indistinguishable from other vesicular compartments at the light microscope level (Segev *et al.*, 1988; Cleves *et al.*, 1991; Franzusoff *et al.*, 1991a; Redding *et al.*, 1991). Although colocalization of Golgi markers by immunofluorescence (Cleves *et al.*, 1991; Franzusoff *et al.*, 1991a) and subcellular fractionation (Abeijon *et al.*, 1989; Cleves *et al.*, 1991) is suggestive of association within the same organelle, these techniques give few clues about the subcompartmental organization of the Golgi complex. Its subcompartmental organization is largely inferred from the accumulation of kinetic intermediates in *sec* mutants; these define functional rather than physical subcompartments (Franzusoff and Schekman, 1989; Graham and Emr, 1991). However, recent studies have separated pairwise, Golgi markers KEX2 and GDPase (Bowser and Novick, 1991; Cunningham and Wickner, 1989) by subcellular fractionation, biochemically defining these subcom-

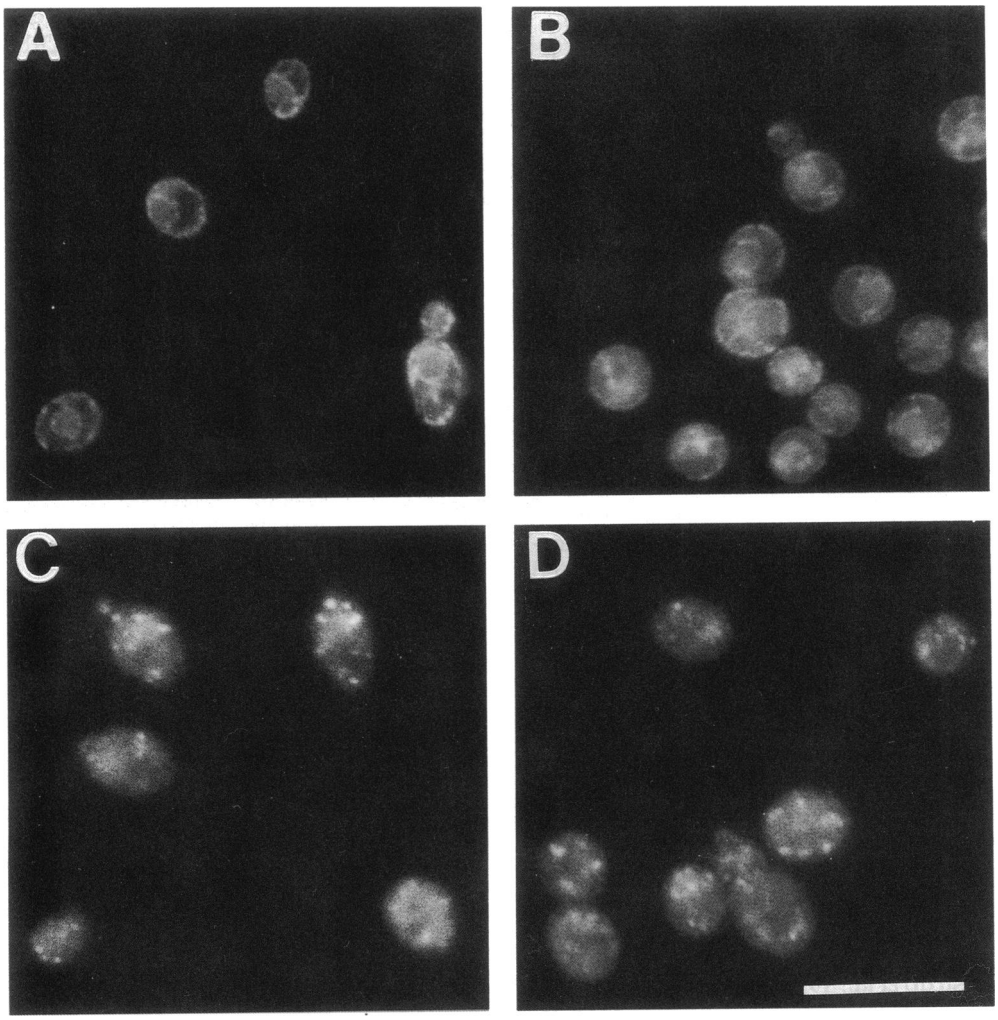

Figure 12. Staining by indirect immunofluorescence of KAR2 and SEC7 in *PMR1* and *pmr1* backgrounds. Strains growing logarithmically in YPD were fixed, permeabilized, labeled with anti-KAR2 or anti-SEC7 antisera, and stained with affinity purified DTAF-conjugated goat anti-rabbit IgG. (A and B) Staining of KAR2 in *PMR1* (AA305) and *pmr1* (AA522) backgrounds, respectively. (C and D) Staining of SEC7 in *PMR1* (AA662) and *pmr1* (AA522) backgrounds, respectively (bar = 10 μm).

partments as distinct physical entities. Thus the novel distribution of PMR1 in relation to known Golgi markers could suggest localization to a Golgi subcompartment, to other organelles such as intermediate vesicles, secretory vesicles, endosomes, or even a less well-defined compartment, such as the calciosome (Volpe, 1988). What our data most clearly demonstrate is where PMR1 is not; it is absent from the ER, PM, and the vacuole. Nonetheless, the weight of available evidence is consistent with partial localization to the Golgi complex, with the possibility that a proportion of PMR1 resides in multiple secretory compartments. The localization of a Ca^{2+}-ATPase to the Golgi is not without precedent (Virk *et al.*, 1985).

The assignment of PMR1 to the Golgi helps to explain some of the phenotypes of the *pmr1* mutant. Our assumption is that PMR1 is required for pumping Ca^{2+} into the lumen of one of the Golgi subcompartments. Accordingly loss of PMR1 from the Golgi membrane could lead to a depletion of the lumenal Ca^{2+} content of the Golgi, an increase in cytosolic Ca^{2+}, or both. That several Golgi processing steps are perturbed is consistent with the notion that Ca^{2+} is required in the Golgi lumen for the full activity of Ca^{2+}-dependent enzymes. We find that the proteolytic maturation of α factor, an event thought to take place in a late Golgi compartment (Julius *et al.*, 1984), is incomplete (Figure 9). This phenotype may reflect a reduction in the activity of KEX2, a Ca^{2+}-dependent Golgi-localized endoprotease (Fuller *et al.*, 1989; Franzusoff *et al.*, 1991a; Redding *et al.*, 1991), because its specific activity is decreased threefold in *pmr1* extracts (Table 5). The sorting of carboxypeptidase Y from the Golgi to the vacuole is only slightly altered, suggesting that vacuolar targeting of proteins is not sig-

Table 5. Specific activity of markers for various compartments in *PMR1* and *pmr1* strains (from the gradients diagrammed in Figure 11)

Marker	Specific activity	
	PMR1 (AA662)	*pmr1* (AA522)
GDPase	71.9	78.9
NADPH cytochrome c reductase	0.0493	0.0488
α mannosidase	2.58	8.76
KEX2	10.7	3.39

Specific activity is expressed as the total number of units (summed over the whole gradient) per milligram protein.

nificantly affected (Figure 10). In contrast, the sorting and retention of heterologous secretory proteins normally trapped within the cell is so profoundly disrupted in *pmr1* that these proteins are secreted into the medium at 5–50-fold higher levels than wild type (Rudolph *et al.*, 1989; Smith *et al.*, 1985). The locus of heterologous protein retention is thought to be the ER, based on the core-like glycosylation pattern of unsecreted proteins in wild-type strains (Moir and Dumais, 1987). However, the localization of PMR1 to a compartment downstream from the ER appears to place the sorting of heterologous proteins as a post-ER event or implies a coupling between the Ca^{2+} content of the ER and downstream compartments. In animal cells, agents that perturb the lumenal Ca^{2+} concentration of secretory compartments (A23187, BAPTA) or inhibit Ca^{2+}-ATPase activity [thapsigargin (Thastrup *et al.*, 1990)] induce the secretion of certain mutant T-cell receptor α chains that are normally retained in the ER (Suzuki *et al.*, 1991), a phenotype reminiscent of the *pmr1*-dependent secretion of heterologous proteins. Ca^{2+}-influenced retention may function through the ER lumenal chaperonin, BiP, as its association with these mutant proteins is Ca^{2+} dependent (Suzuki *et al.*, 1991).

The glycosylation defect exhibited by *pmr1* strains is also consistent with the localization of PMR1 function to the Golgi. The pattern of invertase glycosylation in double mutant combinations of *pmr1* with *sec18*, *ypt1*, and *sec6* delimits the *pmr1* glycosylation defect to the Golgi (Figure 6). This deficiency could result in part from impaired activity of GDPase, a Golgi-localized, Ca^{2+}-requiring enzyme necessary for glycosylation (Abeijon *et al.*, 1989; P. Robbins, personal communication). Invertase secreted from *pmr1* strains receives both α1,6 and α1,3 mannose linkages, hallmarks of early and late Golgi processing steps, respectively (Figure 7). This result implies that secretory proteins are reaching early and late Golgi compartments. However, the truncated glycosylation pattern suggests that the extent of glycosylation on individual molecules is reduced and may indicate impaired outer chain elongation, which is postulated to occur in intermediate Golgi compartments (Franzusoff and Schekman, 1989). Other laboratories see reduced amounts of α1,3 mannose linkages within the population of total invertase isolated from *pmr1* strains (M. Rose, personal communication). This discrepancy may reflect differences in strain background or growth conditions because we have only observed slight reductions in repeated experiments.

A striking characteristic of many *pmr1* phenotypes is their Ca^{2+}-conditional nature. Addition of external calcium to a *pmr1* mutant partially reverses some secretory

Table 6. Summary of the genetic suppression with *pmr1* and lethal overexpression of *PMR1* in *sec* mutants

Strain	Relevant genotype	Suppression by *pmr1*	Lethal over-expression of *PMR1*
Post-Golgi *sec* mutants			
NY768	*sec1-1*	+/− (34°C)	− (32°C)
NY770	*sec2-41*	−	− (34°C)
NY772	*sec3-2*	−	+
NY774	*sec4-8*	−	+
NY776	*sec5-24*	−	+
NY778	*sec6-4*	+++ (36°C)	− (34°C)
NY780	*sec8-9*	−	+
NY782	*sec9-4*	−	−−− (32°C)
NY784	*sec10-2*	−	−−− (37°C)
NY786	*sec15-1*	+ (37–38°C)	− (36°C)
ER/Golgi *sec* mutants			
AA482	*sec 7-1*	−	+
AA471	*sec12-4*	−	+
AA473	*sec13-1*	+/− (34°C)	−− (32°C)
AA474	*sec16-2*	−	+
AA476	*sec17-1*	−	+
AA459	*sec18-1*	−	+
AA468	*sec19-1*	+++ (36°C)	− (34°C)
AA479	*sec20-1*	−	+
AA466	*sec21-1*	−	−−− (32°C)
AA465	*sec22-3*	−	+
AA480	*sec23-1*	−	−− (30°C)
AA311	*ypt1-1*	+++ (14°C)	−−− (22°C)
ANY119	*bet2-1*	−	N.D.
Early *sec* mutants			
L2851	*sec53-6*	−	+
RSY455	*sec61-3*	−	N.D.
RSY530	*sec62*	−	N.D.
RSY153	*sec63-1*	−	N.D.

For suppression, +++ = vigorous growth, somewhat less than wild type. The other symbols (++ and +) represent, respectively, decreasing amounts of growth relative to +++; +/− = variable or very weak suppression; − = no suppression. Temperature of suppression is in parentheses. For lethal overexpression, growth was observed over 1–4 d. −−− = strong synthetic lethality (3–4 logs difference in growth inhibition by PMR1/2μ relative to YEP24 transformed control strains); −− = moderate synthetic lethality (~2 logs difference in growth inhibition relative to controls); − = weak, but noticeable synthetic lethality (~1 log difference in growth inhibition relative to controls); + = no clearcut synthetic lethality. The temperature on the right indicates the semipermissive temperature at which lethal overexpression is most clearly seen. N.D., not determined.

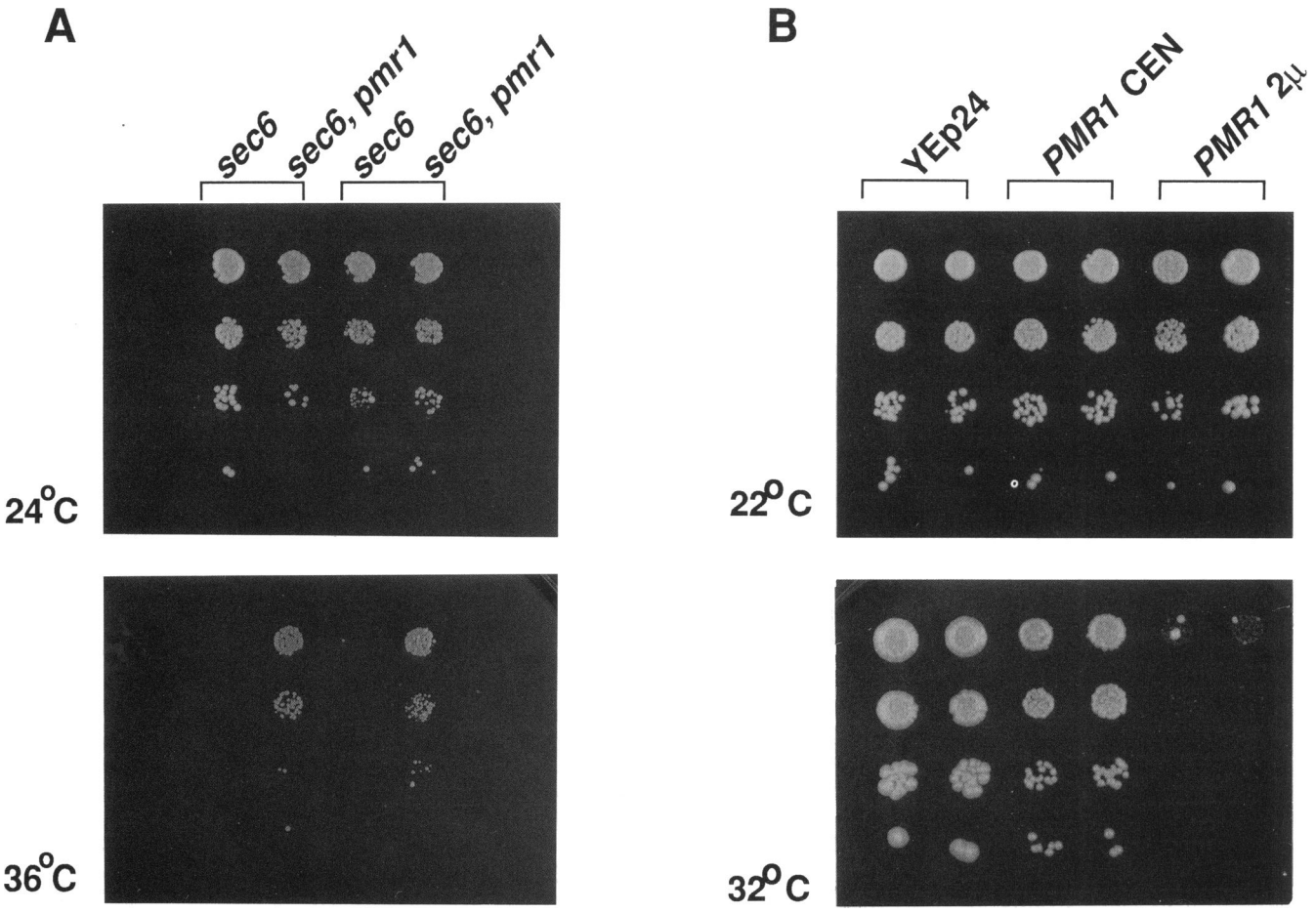

Figure 13. Genetic interactions with *sec* mutants. (A) *pmr1* suppresses the temperature-sensitive lethality of *sec6-4*. Two sets of isogenic pairs, *sec6-4* and *sec6-4 pmr1*, indicated by the brackets, were constructed by transforming *sec6-4 pmr1* double mutant strains AA688 and AA691 with either *PMR1*/CEN (pL149) or control plasmid (pUN80). Equal OD_{600} units of logarithmically growing cells were harvested, serially diluted 10-fold and transferred onto SC-ura media with a pronged inoculator. Top: growth at the permissive temperature of 24°C. Bottom: growth at 36°C, the nonpermissive temperature for the *sec6-4* single mutant. (B) PMR1 overexpression on a 2μ plasmid intensifies the temperature-sensitive growth defect of *sec21-1*. Strain AA466 (*sec21-1*) was transformed with plasmids pL129 (*PMR1*/2μ), pL149 (*PMR1*/CEN), and control plasmid YEp24. Strains were grown to logarithmic phase in SC-ura medium. Equal OD_{600} units of logarithmically growing cells were harvested, serially diluted 10-fold and transferred onto SC-ura media with a pronged inoculator. Top: growth at the permissive temperature of 22°C. Bottom: growth at the semipermissive temperature of 32°C. Brackets indicate pairs of independent transformants.

defects, including outer chain glycosylation of invertase, proteolytic processing of pro-α factor, the sorting of CPY, and secretion of the heterologous protein bovine prochymosin (Don Moir, personal communication). The partial reversal of these secretory defects by Ca^{2+} strongly suggests that a fundamental defect of the *pmr1* mutant results from altered Ca^{2+} balance and is consistent with its proposed role as a Ca^{2+} pump. This reversibility could be explained if the presence of extracellular Ca^{2+} drives more Ca^{2+} into Golgi compartments, thereby restoring Ca^{2+}-dependent events. These results suggest a role for Ca^{2+} itself in the proper function of the Golgi apparatus and normal passage through the secretory pathway. Our finding that a deletion of *pmr1* can suppress *sec* mutations impaired in ER/Golgi transit (*ypt1-1*) (Schmitt *et al.*, 1988; Segev *et al.*, 1988; Bacon *et al.*, 1989; Baker *et al.*, 1990) and post-Golgi transit (*sec6-4*, *sec15-1*), as well as those defective in multiple functions (*sec19-1*) (Novick *et al.*, 1980; Esmon *et al.*, 1981; Bowser and Novick, 1991) also implies a global effect on secretory transport by altered calcium balance (Figure 13, Tables 6 and 7). In these *sec* strains, a decrease of Ca^{2+} in the Golgi lumen or an increase of Ca^{2+} in the cytoplasm caused by the *pmr1* mutation could drive a reaction that otherwise would not take place in *PMR1*. Similarly, overexpression of PMR1 may restrict certain *sec* mutants by limiting a Ca^{2+}-dependent reaction. In support of this idea, YPT1 function in in vitro ER/Golgi transit is closely coupled to a Ca^{2+}-dependent step (Baker *et al.*, 1990), and peptides corresponding to the ras-related rab effector domain potently inhibit ER/Golgi transport at a step coincident with the accumu-

Table 7. Calcium-related interactions of *pmr1* and *sec* mutants

	pmr1 and *sec19-1*			*pmr1* and *ypt1-1*	
	YPD	YPD + Ca^{2+}		EGTA	EGTA + Ca^{2+}
PMR1	+++	+++	*PMR1*	+++	+++
pmr1	+++	+++	*pmr1*	−	+++
sec19-1	−	+	*ypt1-1*	++	++
sec19-1, pmr1	++	−	*ypt1-1, pmr1*	+	++

Strains were patched onto YPD and grown under permissive conditions. Cells were diluted to 5–10 $\times 10^6$ cells/ml in water and replica plated onto various media with a multipronged inoculator. For interactions between *pmr1* and *sec19-1*, strains were replica plated onto YPD and YPD containing 10 mM $CaCl_2$ and incubated at the nonpermissive temperature (36°C) of *sec19-1*. KCl or NaCl did not rescue the *sec19-1* temperature-sensitive growth defect. For interactions between *pmr1* and *ypt1-1*, strains were replica plated onto SC + 25 mM EGTA and SC + 25 mM EGTA + 10 mM $CaCl_2$ and incubated at 30°C. Growth was scored after 2–3 d. +++ = vigorous growth, ++ = moderate growth, + = weak growth, − = poor growth. Each additional plus represents approximately a 5–10-fold increase in cell density.

lation of a Ca^{2+}-dependent prefusion intermediate (Plutner *et al.*, 1990). The interaction of *PMR1* with *sec* mutants from several points in the secretory pathway could also indicate functional and physical localization to more than one secretory compartment.

An alternative to the model that processing and sorting enzymes are Ca^{2+} dependent is that these enzymes or secretory proteins themselves are missorted in a *pmr1* mutant. This mislocalization could result in a loss of normal Golgi subcompartmentalization. In subcellular fractionation and immunofluorescence experiments carried out in *pmr1* strains, we have not found a dramatic mislocalization of internal components (markers for the Golgi and the ER for example do not apparently redistribute to other organelles; see Figures 11 and 12). A rigorous test of this alternative hypothesis will depend on a clearer identification of Golgi subcompartments through subcellular fractionation and immunoelectron microscopy.

ACKNOWLEDGMENTS

We are grateful to D. Preuss for the generous gift of anti-invertase antiserum; A. Franzusoff for the gift of *sec7* and *mnn1* strains, anti-α factor antiserum, anti-SEC7 antiserum, and antiserum directed against α1,6 and α1,3 mannose linkages; P. Novick and S. Ferro-Novick for providing various *sec* mutant strains; R. Schekman, S. Saunders, and C. Kaiser for various *sec* mutant strains and antibody reagents; P. Robbins and P. Orlean for the generous gifts of endoglycosidase H and anti-dol-P-man-synthase antisera; J. Teem for anti-PMA1 monoclonal antibody; M. Rose and J. Vogel for the kind gift of anti-KAR2 antibody; R. Fuller and K. Redding for the gifts of *KEX2* plasmids and anti-KEX2 antiserum. Special thanks goes to P. Ljungdahl, H. Rudolph, S. Kron, L. Davis, K. Cunningham, R. Fuller, and A. Franzusoff for helpful discussions. We thank K. Cunningham, D. Pellman, and C. Kaiser for critical reading of the manuscript. A.A. was supported by a NIH-NRSA predoctoral training grant. G.R.F. is American Cancer Society Professor of Genetics. This work was supported by NIH Grants GM-40266 and GM-35010. The costs of publication of this article were defrayed in part by the payment of page charges. This article must therefore be hereby marked "advertisement" in accordance with 18 U.S.C. Section 1734 solely to indicate this fact.

REFERENCES

Abeijon, C., Orlean, P., Robbins, P.W., and Hirschberg, C.B. (1989). Topography of glycosylation in yeast: characterization of GDPmannose transport and lumenal guanosine diphosphatase activities in Golgi-like vesicles. Proc. Natl. Acad. Sci. USA *86*, 6935–6939.

Bacon, R.A., Salminen, A., Ruohola, H., Novick, P., and Ferro, N.S. (1989). The GTP-binding protein Ypt1 is required for transport in vitro: the Golgi apparatus is defective in ypt1 mutants. J. Cell Biol. *109*, 1015–1022.

Baker, D., Wuestehube, L., Schekman, R., Botstein, D., and Segev, N. (1990). GTP-binding Ypt1 protein and Ca^{2+} function independently in a cell-free protein transport reaction. Proc. Natl. Acad. Sci. USA *87*, 355–359.

Beckers, C.J., and Balch, W.E. (1989). Calcium and GTP: essential components in vesicular trafficking between the endoplasmic reticulum and Golgi apparatus. J. Cell Biol. *108*, 1245–1256.

Booth, C., and Koch, G.L. (1989). Perturbation of cellular calcium induces secretion of luminal ER proteins. Cell *59*, 729–737.

Bowser, R., and Novick, P. (1991). Sec15 protein, an essential component of the exocytotic apparatus, is associated with the plasma membrane and with a soluble 19.5S particle. J. Cell Biol. *112*, 1117–1131.

Bradford, M.N. (1976). A rapid and sensitive method for the quantitation of microgram quantities of protein utilizing the principle of protein-dye binding. Anal. Biochem. *72*, 248–254.

Burgoyne, R.D. (1987). G proteins: control of exocytosis [news]. Nature *328*, 112–113.

Burk, S.E., Lytton, J., MacLennan, D.H., and Shull, G.E. (1989). cDNA cloning, functional expression, and mRNA tissue distribution of a third organellar Ca^{2+} pump. J. Biol. Chem. *264*, 18561–18568.

Carafoli, E. (1987). Intracellular calcium homeostasis. Annu. Rev. Biochem. *56*, 395–434.

Carafoli, E. (1991). Calcium pump of the plasma membrane. Physiol. Rev. *71*, 129–153.

Cleves, A.E., McGee, T.P., Whitters, E.A., Champion, K.M., Aitken, J.R., Dowhan, W., Goebl, M., and Bankaitis V.A. (1991). Mutations in the CDP-choline pathway for phospholipid biosynthesis bypass the requirement for an essential phospholipid transfer protein. Cell *64*, 789–800.

Cunningham, K.W., and Wickner, W.T. (1989). Yeast KEX2 protease and mannosyltransferase I are localized to distinct compartments of the secretory pathway. Yeast *5*, 25–33.

Davis, L.I., and Fink, G.R. (1990). The *NUP1* gene encodes an essential component of the yeast nuclear pore complex. Cell *61*, 965–978.

deCurtis, I., and Simons, K. (1988). Dissection of Semliki Forest virus glycoprotein delivery from the trans-Golgi network to the cell surface in permeabilized BHK cells. Proc. Natl. Acad. Sci. USA *85*, 8052–8056.

Deshaies, R.J., and Schekman, R. (1987). A yeast mutant defective at an early stage in import of secretory protein precursors into the endoplasmic reticulum. J. Cell Biol. *105*, 633–645.

Elion, E.A., Grisafi, P., and Fink, G.R. (1990). FUS3 Encodes a cdc2+/CDC28-related kinase required for the transition from mitosis into conjugation. Cell *60*, 649–664.

Elledge, S.J., and Davis, R.W. (1988). A family of versatile centromeric vectors designed for use in the sectoring-shuffle mutagenesis assay in *Saccharomyces cerevisiae*. Gene *70*, 303–312.

Esmon, B., Novick, P., and Schekman, R. (1981). Compartmentalized assembly of oligosaccharides on exported glycoproteins in yeast. Cell *25*, 451–460.

Feldman, R.I., Bernstein, M., and Schekman, R. (1987). Product of SEC53 is required for folding and glycosylation of secretory proteins in the lumen of the yeast endoplasmic reticulum. J. Biol. Chem. *262*, 9332–9339.

Field, J., Nikawa, J., Broek, D., MacDonald, B., Rodgers, L., Wilson, I.A., Lerner, R.A., and Wigler, M. (1988). Purification of a RAS-responsive adenylyl cyclase complex from *Saccharomyces cerevisiae* by use of an epitope addition method. Mol. Cell. Biol. *8*, 2159–2165.

Franzusoff, A., Redding, K., Crosby, J., Fuller, R.S., and Schekman, R. (1991a). Localization of components involved in protein transport and processing through the yeast Golgi apparatus. J. Cell Biol. *112*, 27–37.

Franzusoff, A., Rothblatt, J., and Schekman, R. (1991b). Analysis of polypeptide transit through yeast secretory pathway. Methods Enzymol. *194*, 662–674.

Franzusoff, A., and Schekman, R. (1989). Functional compartments of the yeast Golgi apparatus are defined by the *sec7* mutation. EMBO J. *8*, 2695–2702.

Fuller, R.S., Brake, A., and Thorner, J. (1989). Yeast prohormone processing enzyme (KEX2 gene product) is a Ca^{2+}-dependent serine protease. Proc. Natl. Acad. Sci. USA *86*, 1434–1438.

Fuller, R.S., Sterne, R.E., and Thorner, J. (1988). Enzymes required for yeast prohormone processing. Annu. Rev. Physiol. *50*, 345–362.

Goud, B., Salminen, A., Walworth, N.C., and Novick, P.J. (1988). A GTP-binding protein required for secretion rapidly associates with secretory vesicles and the plasma membrane in yeast. Cell *53*, 753–768.

Graham, T.R., and Emr, S.D. (1991). Compartmental organization of Golgi-specific protein modification and vacuolar protein sorting events defined in a yeast *sec18* (NSF) mutant. J. Cell Biol. *114*, 207–218.

Gunteski-Hamblin, A., Greeb, J., and Shull, G.E. (1988). A novel Ca^{2+} pump expressed in brain, kidney, and stomach is encoded by an alternative transcript of the slow-twitch muscle sarcoplasmic reticulum Ca^{2+}-ATPase gene. Identification of cDNAs encoding Ca^{2+} and other cation-transporting ATPases using an oligonucleotide probe derived from the ATP-binding site. J. Biol. Chem. *263*, 15032–15040.

Hanahan, D. (1985). Techniques for transformation of *E. coli*. In: DNA Cloning, ed. D.M. Glover, Oxford, England: IRL Press, *1*, 109–135.

Haslik, A., and Tanner, W. (1978). Biosynthesis of the vacuolar yeast glycoprotein carboxypeptidase Y. Eur. J. Biochem. *85*, 599–608.

Huttner, W.B., Gerdes, H.H., and Rosa, P. (1991). The granin (chromogranin/secretogranin) family. Trends Biochem. Sci. *16*, 27–30.

Ito, H., Fukuda, Y., Murata, K., and Kimura, A. (1983). Transformation of intact yeast cells treated with alkali cations. J. Bacteriol. *153*, 163–168.

Johnson, D.A., Gautsch, J.W., Sportsman, J.R., and Elder, J.H. (1984). Improved technique utilizing nonfat dry milk for analysis of proteins and nucleic acids transferred to nitrocellulose. Gene Anal. Tech. *1*, 3–8.

Julius, D., Brake, A., Blair, L., Kunisawa, R., and Thorner, J. (1984). Isolation of the putative structural gene for the lysine-arginine-cleaving endopeptidase required for processing of yeast prepro-alpha-factor. Cell *37*, 1075–1089.

Kaiser, C.A., and Schekman, R. (1990). Distinct sets of SEC genes govern transport vesicle formation and fusion early in the secretory pathway. Cell *61*, 723–733.

King, S.C., Ellenberger, T.E., and Goldin, S.M. (1988). Biochemical and immunological evidence for a calcium pump in chromaffin granules. Biochem. Biophys. Res. Commun. *155*, 656–663.

Klemper, M.S. (1985). An adenosine triphosphate-dependent calcium uptake pump in human neutrophil lysosomes. J. Clin. Invest. *76*, 303–310.

Klionsky, D.J., Herman, P.K., and S.D. Emr (1990). The fungal vacuole: composition, function, and biogenesis. Microbiol. Rev. *54*, 266–292.

Koerner, T.J., Hill, J.E., Myers, A.M., and Tzagoloff, A. (1991). High-expression vectors with multiple cloning sites for construction of trpE fusion genes: pATH vectors. Methods Enzymol. *194*, 477–490.

Kolodziej, P.A., and Young, R.A. (1991). Epitope tagging and protein surveillance. In: Methods in Enzymology, Guide to Yeast Genetics and Molecular Biology, ed. C.A. Guthrie, G.R. Fink, San Diego: Academic Press, Volume 194, 508–519.

Kunkel, T.A., Roberts, J.D., and Zakour, R.A. (1987). Rapid and efficient site-specific mutagenesis without phenotypic selection. Methods Enzymol. *154*, 367–382.

Laemmli, U.K. (1970). Cleavage of structural proteins during the assembly of the head of bacteriophage T4. Nature *227*, 680–685.

Lodish, H.F., and Kong, N. (1990). Perturbation of cellular calcium blocks exit of secretory proteins from the rough endoplasmic reticulum. J. Biol. Chem. *265*, 10893–10899.

MacLennan, D.H., Brandl, C.J., Korczak, B., and Green, N.M. (1985). Amino-acid sequence of a Ca^{2+} + Mg^{2+}-dependent ATPase from rabbit muscle sarcoplasmic reticulum, deduced from its complementary DNA sequence. Nature *316*, 696–700.

Maniatas, T., Fritsch, E.F., and Sambrook, J. (1982). Molecular Cloning: A Laboratory Manual. Cold Spring Harbor, New York: Cold Spring Harbor Laboratory Press.

Marriott, M., and Tanner, W. (1979). Localization of dolichyl phosphate- and pyrophosphate-dependent glycosyl transfer reactins in *Saccharomyces cerevisiae*. J. Bacteriol. *139*, 565–572.

Milne, J.L., and Coukell, M.B. (1989). Identification of a high-affinity Ca^{2+} pump associated with endocytotic vesicles in *Dictyostelium discoideum*. Exp. Cell Res. *185*, 21–32.

Moir, D.T., and Dumais, D.R. (1987). Glycosylation and secretion of human alpha-1-antitrypsin by yeast. Gene *56*, 209–217.

Nakajima, T., and Ballou, C.E. (1975). Yeast mannoprotein biosynthesis: solubilization and selective assay of four mannosyltransferases. Proc. Natl. Acad. Sci. USA *72*, 3912–3916.

Newman, A.P., and Ferro-Novick, S. (1987). Characterization of new mutants in the early part of the yeast secretory pathway isolated by a [^{3}H]mannose suicide selection. J. Cell Biol. *105*, 1587–1594.

Normington, K., Kohno, K., Kozutsumi, Y., Gething, M.J., and Sambrook, J. (1989). *S. cerevisiae* encodes an essential protein homologous in sequence and function to mammalian BiP. Cell *57*, 1223–1236.

Novick, P., Ferro, S., and Schekman, R. (1981). Order of events in the yeast secretory pathway. Cell *25*, 461–469.

Novick, P., Field, C., and Schekman, R. (1980). Identification of 23 complementation groups required for post-translational events in the yeast secretory pathway. Cell *21*, 205–215.

Ohashi, A., Gibson, J., Gregor, I., and Schatz, G. (1982). Import of proteins into mitochondria. The precursor of cytochrome c1 is processed in two steps, one of them heme-dependent. J. Biol. Chem. *257*, 13042–13047.

Ohya, Y., Ohsumi, Y., and Anraku, Y. (1984). Genetic study of the role of calcium ions in the cell division cycle of *S. cerevesiae*. Mol. Gen. Genet. *193*, 389–394.

Opheim, D.J. (1978). α-D-Mannosidase of *Saccharomyces cerevisiae:* characterization and modulation of activity. Biochim. Biophys. Acta *524*, 121–130.

Orlean, P., Kuranda, M.J., and Albright, C.F. (1991). Analysis of glycoproteins from *Saccharomyces cerevisiae*. Methods Enzymol. *194*, 682–697.

Plutner, H., Schwaninger, R., Pind, S., and Balch, W.E. (1990). Synthetic peptides of the Rab effector domain inhibit vesicular transport through the secretory pathway. EMBO J. *9*, 2375–2383.

Preuss, D., Mulholland, J., Franzusoff, A., Segev, N., and Botstein, D. (1992). Characterization of the *Saccharomyces* Golgi complex through the cell cycle by immunoelectron microscopy. Mol. Biol. Cell (*in press*).

Redding, K., Holcomb, C., and Fuller, R.S. (1991). Immunolocalization of Kex2 protease identifies a putative late Golgi compartment in the yeast *Saccharomyces cerevisiae*. J. Cell Biol. *113*, 527–538.

Roos, N. (1988). A possible site of calcium regulation in rat exocrine pancreas cells: an X-ray microanalytical study. Scanning Microsc. 2, 323–329.

Rose, M.D., Misra, L.M., and Vogel, J.P. (1989). KAR2, a karyogamy gene, is the yeast homolog of the mammalian BiP/GRP78 gene. Cell *57*, 1211–1221.

Rothblatt, J., and Schekman, R. (1989). A hitchhiker's guide to analysis of the secretory pathway in yeast. Methods Cell Biol. *32*, 3–36.

Rothstein, R.J. (1983). One-step gene disruption in yeast. Methods Enzymol. *101*, 202–211.

Rudolph, H.K., Antebi, A., Fink, G.R., Buckley, C.M., Dorman, T.E., LeVitre, J., Davidow, L.S., Mao, J.I., and Moir, D.T. (1989). The yeast secretory pathway is perturbed by mutations in *PMR1*, a member of a Ca^{2+} ATPase family. Cell *58*, 133–145.

Sanger, F., Nicklen, S., and Coulsen, A.R. (1977). DNA sequencing with chain-terminating inhibitors. Proc. Natl. Acad. Sci. USA *74*, 5463–5467.

Schauer, I., Emr, S., Gross, C., and Schekman, R. (1985). Invertase signal and mature sequence substitutions that delay intercompartmental transport of active enzyme. J. Cell Biol. *100*, 1664–1675.

Schmitt, H.D., Puzicha, M., and Gallwitz, D. (1988). Study of a temperature-sensitive mutant of the ras-related YPT1 gene product in yeast suggests a role in the regulation of intracellular calcium. Cell *53*, 635–647.

Schwaninger, R., Beckers, C.J.M., and Balch, W.E. (1991). Sequential Transport of Protein between the endoplasmic reticulum and successive Golgi compartments in semi-intact Cells. J. Biol. Chem. *266*, 13055–13063.

Segev, N., Mulholland, J., and Botstein, D. (1988). The yeast GTP-binding YPT1 protein and a mammalian counterpart are associated with the secretion machinery. Cell *52*, 915–924.

Sherman, F., Hicks, J.B., and Fink, G.R. (1986). Methods in Yeast Genetics. Cold Spring Harbor, New York: Cold Spring Harbor Laboratory Press.

Smith, R.A., Duncan, M.J., and Moir, D.T. (1985). Heterologous protein secretion from yeast. Science *229*, 1219–1224.

Somlyo, A.P., Bond, M., and Somlyo, A.V. (1985). Calcium content of mitochondria and endoplasmic reticulum in liver frozen rapidly in vivo. Nature *314*, 622–625.

Spindler, K.R., Rosser, D.S., and Berk, A.J. (1984). Analysis of adenovirus transforming proteins from early regions 1A and 1B with antisera to inducible fusion antigens produced in *Escherichia coli*. J. Virol. *49*, 132–141.

Streb, H., Bayerdorffer, E., Haase, W., Irvine, R.F., and Schulz, I. (1984). Effect of inositol-1,4,5-trisphosphate on isolated subcellular fractions of rat pancreas. J. Membr. Biol. *81*, 241–253.

Suzuki, C.K., Bonifacino, J.S., Lin, A.Y., Davis, M.M., and Klausner, R.D. (1991). Regulating the retention of T-cell α chain variants within the endoplasmic reticulum: Ca^{2+}-dependent association with BiP. J. Cell Biol. *114*, 189–205.

Thastrup, O., Cullen, P.J., Drobak, B.K., Hanley, M.R., and Dawson, A.P. (1990). Thapsigargin, a tumor promoter, discharges intracellular Ca^{2+} stores by specific inhibition of the endoplasmic reticulum Ca2(+)-ATPase. Proc. Natl. Acad. Sci. USA *87*, 2466–2470.

Vieira, J., and Messing, J. (1987). Production of single-stranded plasmid DNA. Methods Enzymol. *153*, 3–11.

Virk, S.S., Kirk, C.J., and Shears, S.B. (1985). Ca^{2+} transport and Ca^{2+}-dependent ATP hydrolysis by Golgi vesicles from lactating rat mammary glands. Biochem. J. *226*, 741–748.

Volpe, P., Krause, K.H., Hashimoto, S., Zorzato, F., Pozzan, T., Meldolesi, J., and Lew, D.P. (1988). "Calciosome," a cytoplasmic organelle: the inositol 1,4,5-trisphosphate-sensitive Ca^{2+} store of nonmuscle cells? Proc. Natl. Acad. Sci. USA *85*, 1091–1095.

Wileman, T., Kane, L.P., Carson, G.R., and Terhorst, C. (1991). Depletion of cellular calcium accelerates protein degradation in the endoplasmic reticulum. J. Biol. Chem. *266*, 4500–4507.

Wilson, I.A., Niman, H.L., Houghten, R.A., Cherenson, A.R., Connolly, M.L., and Lerner, R.A. (1984). The structure of an antigenic determinant in a protein. Cell *37*, 767–778.